Lawrence Berkeley National Laboratory
Recent Work

Title
CRYSTAL STRUCTURE AND PHYSICAL PROPERTIES OF AMERICIUM METAL

Permalink
https://escholarship.org/uc/item/7zw5s7db

Author
McWhan, Denis Bayman.

Publication Date
1961-05-01

eScholarship.org Powered by the California Digital Library
University of California

UCRL 9695
cy 2

University of California

Ernest O. Lawrence Radiation Laboratory

TWO-WEEK LOAN COPY

This is a Library Circulating Copy which may be borrowed for two weeks. For a personal retention copy, call Tech. Info. Division, Ext. 5545

Berkeley, California

DISCLAIMER

This document was prepared as an account of work sponsored by the United States Government. While this document is believed to contain correct information, neither the United States Government nor any agency thereof, nor the Regents of the University of California, nor any of their employees, makes any warranty, express or implied, or assumes any legal responsibility for the accuracy, completeness, or usefulness of any information, apparatus, product, or process disclosed, or represents that its use would not infringe privately owned rights. Reference herein to any specific commercial product, process, or service by its trade name, trademark, manufacturer, or otherwise, does not necessarily constitute or imply its endorsement, recommendation, or favoring by the United States Government or any agency thereof, or the Regents of the University of California. The views and opinions of authors expressed herein do not necessarily state or reflect those of the United States Government or any agency thereof or the Regents of the University of California.

UCRL-9695
Chemistry General
TID-4500 (16th Ed.)

UNIVERSITY OF CALIFORNIA

Lawrence Radiation Laboratory
Berkeley, California

Contract No. W-7405-eng-48

CRYSTAL STRUCTURE AND PHYSICAL PROPERTIES OF AMERICIUM METAL

Denis Bayman McWhan

(Thesis)

May 1961

Printed in USA. Price $2.25. Available from the
Office of Technical Services
U. S. Department of Commerce
Washington 25, D.C.

CRYSTAL STRUCTURE AND PHYSICAL PROPERTIES OF AMERICIUM METAL

Contents

Abstract 3

I. Introduction 5

II. Preparation of Americium Metal 7

A. Reduction of Americium Trifluoride with Barium . . 9

B. Reduction of Americium Dioxide with Lanthanum . . 22

C. Americium Monoxide 26

D. Attempted Preparation of "Expanded" Americium Metal 27

E. Purity of Americium Metal Samples 29

III. Melting Point of Americium Metal 31

IV. Crystal Structure of Americium Metal

A. Experimental Procedure 34

B. Determination of Accurate Lattice Parameters . . 40

C. Results 48

V. Magnetic Susceptibility Measurements

A. Experimental Procedure 63

B. Results 69

C. Susceptibility of Americium (III) 72

D. Calculated Magnetic Susceptibility of Plutonium (III) and Americium (III) 75

VI. Variation of the Electrical Resistivity with Temperature and Pressure 84

VII. Discussion 87

Acknowledgments 98

References 99

CRYSTAL STRUCTURE AND PHYSICAL PROPERTIES OF AMERICIUM METAL

Denis Bayman McWhan

Lawrence Radiation Laboratory
University of California
Berkeley, California

May 1961

ABSTRACT

The methods for preparing milligram quantities of pure, well crystallized americium metal are discussed in detail. A versatile high and low temperature x-ray powder camera for small radioactive samples is presented.

Americium metal prepared by the reduction of americium trifluoride with barium vapor has been indexed as hexagonal close-packed with $a = 3.4681 \pm 0.0008$ A and $c = 11.240 \pm 0.005$ A at 20°C. The proposed structure type is that of lanthanum metal ($P6_3/mmc$ with metal atoms in 2(a) 000; $00\frac{1}{2}$ and 2(c) 1/3, 2/3, 1/4; 2/3, 1/3, 3/4). Americium metal condensed on a tantalum wire or quartz fiber from the vapor phase was found to be face-centered cubic ($a = 4.895 \pm 0.005$) A, with a density similar to the dhcp structure. Attempts to reproduce the low density double hexagonal close-packed structure with $a = 3.642 \pm 0.005$ A and $c = 11.76 \pm 0.01$ A reported in the literature have failed. Evidence for the existence of a face-centered cubic form of americium metal above 600°C, is presented.

The following physical properties of americium metal have been determined:

1. Melting point: 995 ± 4°C.
2. Density (x-ray): 13.671 ± 0.005 gm/cm^3 (20°C).
3. Metallic radius (CN 12): 1.730 A.

4. Coefficient of thermal expansion: (20^{o}C)

$$a_a = 7.5 \pm 0.2 \times 10^{-6}\ {}^{o}C^{-1}$$

$$a_c = 6.2 \pm 0.4 \times 10^{-6}\ {}^{o}C^{-1}$$

calculated from:

$$a_T = 3.4672 + 2.60 \times 10^{-5}T + 0.54 \times 10^{-8}T^2 (\sigma = 0.001)$$

$$c_T = 11.237 + 6.95 \times 10^{-5}T + 6.8 \times 10^{-8}T^2 (\sigma = 0.005)$$

$$(-121 \leq T \leq 605^{o}C)$$

5. Magnetic susceptibility: $\chi = (881 \pm 46) \times 10^{-6}$ erg/gauss^2/mole

$\frac{\Delta\chi}{\chi}$ $\begin{cases} \leq 2\% \text{ from 20 to } -196^{o}C \\ \leq 5\% \text{ from 20 to } 550^{o}. \end{cases}$

The magnetic susceptibility of Am^{+3} in americium trifluoride has been determined: χ_m = (566, 564, 567, and 848)$\times 10^{-6}$ cgs units at 20, 0, -72, -196^{o}C, respectively. The susceptibility of Pu^{+3} and Am^{+3} have been calculated making a correction for the estimated departure from Russell-Saunders coupling caused by the spin orbit interaction. For Pu^{+3} the calculated susceptibility is in agreement with the susceptibility of Pu^{+3} in $PuCl_3$ reported in the literature. ($\chi_{M,\,calc.} = 628 \times 10^{-6}$ and $\chi_{M,\,obs.} = 657 \times 10^{-6}$ cgs units at 300^{o}K). The susceptibility of Am^{+3} has been calculated as $\chi_M = 682 \times 10^{-6}$ cgs units, independent of temperature below 500^{o}K.

I. INTRODUCTION

Extensive studies are being made to elucidate the nature of the metallic bond in the heavy element region. In comparison with the more common metals, the heavy metals--uranium, neptunium, and plutonium--all exhibit anomalous physical properties. For example, they have quite complex room temperature crystal structures instead of the simple ones (hexagonal close-packed, face-centered cubic, or body-centered cubic) found in most metals. To date, the anomalous magnetic, electrical, and dilatometric properties of plutonium have not been given a satisfactory theoretical explanation.

In comparison with the earlier members of the series, only a modest amount of work has been done on americium metal. It was first made by Westrum and Eyring, using methods similar to those used in the preparation of plutonium and neptunium.[1] Previously reported physical properties of americium metal are listed in Table I. It should be emphasized that the metal used in making these measurements was not well characterized. The investigators used spectrographic analysis, which is a sensitive test only for cationic impurities; In most cases, x-ray diffraction patterns obtained from the polycrystalline samples were poor and uninterpreted. The crystal structure of americium metal has been reported by Graf et al. to be double hexagonal close-packed, dhcp (space group $P6_3/mmc$, a = 3.642 ± 0.005 A and c = 11.76 ± 0.01 A) similar to the early members of the rare earch series.[4] These workers also measured the magnetic susceptibility and report $\chi_{300^\circ K} = 1000 \pm 250 \times 10^{-6}$ erg/gauss^2/mole. L. B. Asprey[5] has prepared americium metal with a face-centered cubic structure (a = 4.89 A). The density of the latter metal is 16% greater than that prepared by Graf, thus leading to the speculation that americium metal might be similar to cerium metal, which exhibits a "collapsed" phase at low temperatures.

Table I. Physical properties of americium metal

	Reference
1. Density: 11.7 ± 0.3 g/cm^3	1
2. Melting point: Softening at 850 °C, but incomplete even at 1200 °C	2
3. Vapor pressure: $\log(p_{mm}) = 7.563 - 13{,}162/T$ ($1103\ ^{\circ}K \leq T \leq 1453\ ^{\circ}K$)	2
4. Boiling point: 2880 °K	2
5. Heat of vaporization: 57 kcal/mole (2880 °K)	2
6. Heat of solution: (1.5 M HCl) -162.3 ± 2.7 kcal/mole Am	3

In the following work the methods for preparing milligram quantities of pure, well crystallized metal are discussed in detail. In an attempt to characterize americium metal the following physical properties have been studied:

1. the melting point has been determined, by using a new technique suitable for reactive metal samples as small as 10 to 20 μ g.
2. the crystal structure and coefficient of thermal expansion have been determined from -120°C to 600°C; for these measurements a versatile high- and low-temperature powder camera for small radioactive samples was designed.
3. the magnetic susceptibility has been measured from -196 to 550°C.
4. the variation in the electrical resistivity with temperature and pressure has been studied.

These properties are discussed in the light of the properties of the other actinide and rare earth metals.

II. PREPARATION OF AMERICIUM METAL

The preparation of pure, well crystallized lanthanide and actinide metals has proved a formidable task. The heat of formation of their compounds is very high, and, consequently, attempts to make the metals by classical techniques have failed. An excellent review of the history of the rare earth metals has been written by Trombe.[6] He points out that the metals are very reactive and that it is even difficult to find materials from which to make crucibles. During the Second World War exhaustive studies were made on the preparation of plutonium metal. The methods devised in the Metallurgical Laboratory have been summarized by Fried et al.[7] They centered around the reduction of an actinide fluoride with an alkali or alkaline earth metal. The reductions were carried out in a double crucible system made of a refractory oxide such as beryllia or thoria, and the crucible system was heated in vacuum by resistance heating.

Americium metal was first made by Westrum and Eyring, using these techniques.[1] They reduced microgram quantities of americium trifluoride with barium vapor in a beryllia double crucible system at 1100°C for 1.5 min at a pressure of 10^{-6} mm. The small globules of metal obtained in these reductions were used to measure the density and heat of solution (in 1.5 M HCl) of americium metal.

Wallmann and Cunningham indicate that in their work these methods were seldom more than 50% successful with americium, because the product often soaks into the refractory oxide crucible.[8] As a result of their experiments, they suggest using an all-tantalum double crucible system and a wet precipitated fluoride. The former leads to more reproducible reduction conditions, and the latter is easier to handle on the microgram scale than fluoride prepared by hydrofluorination. They also find it more convenient to use induction heating.

In preparing metal for his crystallographic studies, Graf used a tantalum crucible system and carried out the reductions at 1300°C for 0.5 minute and 1130°C for 3 minutes.[4] The product was then

annealed for 4 hours at 800°C and cooled to room temperature at a rate of 1.8° to 2° per minute.

An entirely different approach to the preparation of americium metal has been made by Asprey,[5] using a method developed by Daane et al.[9] for the preparation of the more volatile rare earth metals. Americium oxide was reduced with lanthanum metal at 1200°C. The large difference in the volatility of americium and lanthanum metals allows the product to be separated by distillation. The americium was effused through a hole in the crucible cap and collected on a quartz fiber located above the effusion orifice.

The diversity in methods of preparing americium metal and the difference in the crystal structure of metal made by the last two techniques indicate that a careful study of the variables involved in the preparation and recovery of pure, well crystallized metal is needed. Such a study has been under way in this Laboratory for several years, and some results are presented in the following work. The variables that will be considered are

(1) choice of reductant metal,
(2) physical form and treatment of starting materials,
(3) type of crucible system,
(4) reduction temperature and duration of reduction,
(5) effect of annealing and cooling rate,
(6) method of heating.

Before one can discuss these points, the criterion for a successful reduction must be established. Of prime importance is the purity of the metal. Spectrographic analysis is used to detect traces of cationic impurities, but, as pointed out in the introduction, it is of little or no use in the detection of anionic impurities on our scale. Unfortunately, at present, there is no convenient way of detecting trace quantities of the light nonmetals such as oxygen and nitrogen in submilligram samples of heavy metals. (One mole % of oxygen in americium is only 0.05 weight %. Therefore, to limit the amount of oxygen in a 1-mg sample to even 1 mole % would require the detection of 0.7 μg

of oxygen.) Trace amounts of anionic impurities have been reported to stabilize normally unstable phases in metals. For example, in ytterbium an hexagonal close-packed structure instead of the normal face-centered-cubic structure was observed when an oxide coat had formed on the metal in high-temperature x-ray studies.[10] Gross contamination with anionic impurities leads to the formation of interstitial compounds. These compounds have a metallic luster but are brittle.[11] Malleability, therefore, is a test for gross contamination. The influence of minor amounts of impurities in stabilizing certain crystalline structures probably can be neglected if all samples of metal made under widely differing conditions yield the same structure. X-ray powder patterns will be used as a criterion not only to show that the same structure is reproduced but also to measure how well crystallized the sample is. Finally, it is desirable to have the product in the form of a single globule of metal which is easily removed from the reduction crucible.

In the following sections, the two general types of reactions used to prepare americium metal,

$$AmF_3 + (3/x)M \rightleftharpoons Am + (3/x)MF_x ,$$

and

$$3AmO_2 + 4La \rightleftharpoons 3Am + 2La_2O_3 ,$$

are considered in the light of the above discussion. The attempts made to reproduce the crystal structure proposed by Graf et al.[4] are summarized; the problem of americium monoxide is discussed; and the samples used in the study of the physical properties are described.

A. Americium Trifluoride Reductions

The preparation of americium metal by the reduction of americium trifluoride is more difficult than the similar reactions with neptunium or plutonium because of two factors:

(a) the melting point of americium is 355°C higher than that of neptunium or plutonium, thus reducing to approximately 100°C the temperature difference between the melting point and the temperature at which the product wets the crucible;

(b) americium is more volatile.

This means that a delicate balance of conditions must be maintained to obtain reasonable yields of recoverable metal, and, consequently, the conditions must be reproducible.

1. Reductant Metal

The choice of reductant metal is limited by two factors:

(a) the ΔF for the reaction must be thermodynamically favorable;

(b) the vapor pressure of the reductant metal must be sufficiently high to permit vaporization of the excess in a reasonable time without a substantial loss of americium.

Table II lists some reductant metals that satisfy these criteria as shown by the vapor pressure and estimated free energies for the reaction

$$AmF_3 + (3/x)M \rightleftharpoons Am + (3/x)MF_x .$$

Lithium, calcium, and barium are possible reductants, and the choice among them is somewhat arbitrary. If lithium is used, the lithium fluoride formed in the reaction vaporizes along with the excess lithium, leaving only americium metal as the product. The americium can then be used with little or no subsequent handling. This is especially desirable when only very small quantities of the actinide fluoride are available, as in the case of transamericium elements. Also, the chance of contamination of the product with ferromagnetic impurities resulting from handling and cleaning is reduced; this is an important consideration if magnetic studies are contemplated. However, if barium or calcium

Table II. Thermodynamics of AmF_3 reductions

Reductant	x	ΔF_T (kcal/gram-atom AmF_3)[12]			v. p. (mm)[13]			$T^\circ K$, where v. p. of MF_x is 10^{-3} atm.[14]
		1000°K	1250°K	1500°K	1000°K	1250°K	1500°K	
Li	1	-9	-36	-30	1	30	400	1304
Na	1	-9	+3	+21	180	above b. p.		1322
K	1	-3	+12	+27	650	above b. p.		1142
Ca	2	-48	-45	-39	0.2	10	100	1690
Ba	2	-42	-42	-39	0.1	5	70	1870

T (in °K	1000	1250	1500
v. p. of Am (in mm)	3×10^{-6}	10^{-3}	0.05

is used, the barium fluoride or calcium fluoride slag provides a protective coating against surface reactions with the residual gases in the system during annealing, and tends to isolate the product from the crucible, making removal of the product easier. Moreover, even a small weight percent of light elements may constitute a high mole percent impurity [0.01 wt % Li = 3.5 mole %, 0.1 wt % Ba =0.2 mole % (in americium)] . As the purity of the americium metal is of major importance, the author has used barium preferentially as the reductant, although lithium has also been used in several successful reductions.

2. Physical Form and Treatment of Starting Materials

The first problem in the preparation of americium trifluoride is that of assuring its freedom from cationic impurities. Because of the scale on which this work had to be done, ordinary reagents were not pure enough. The Am^{241} used in this study was obtained from Oak Ridge in the form of a nitrate solution which contained 2 wt % aluminum and 2 wt % calcium as the only spectrographically detectable impurities. These impurities were removed by using a method developed by Naito.[15] The americium was absorbed on the top of a Dowex-50 column, and the aluminum removed by washing with 1 M sodium hydroxide. The americium and calcium were eluted with 2 M hydrochloric acid. After the calcium was eluted, the americium was stripped with 6 M hydrochloric acid. The purity of the resulting stock solution is limited by that of the reagents. It has been found that it is rather troublesome to obtain pure acids and bases. Pyrex containers cannot be used, as they introduce significant amounts of calcium, aluminum, and magnesium.[16] Consequently, all work was done in quartz or polyethylene containers which had been leached with concentrated hydrochloric acid. Only water distilled in quartz apparatus was used, and the hydrochloric acid solutions were made by bubbling hydrogen chloride gas into this water. With these techniques americium stock solutions containing 0.003 mole of cationic impurities per mole of americium have been obtained.

All the other reagents used in this work were checked for purity. It should be noted that commercial hydrogen fluoride solutions often contain small quantities of aluminum; therefore, hydrofluoric acid solutions were made by vapor equilibration of quartz-distilled water in polyethylene containers.

It is highly desirable that the fluoride be obtained in the form of compact "chunks" rather than in the form powder: first, because powdered material will not yield a single globule of product metal at ordinary reduction temperatures; and, second, to maintain ease of loading in the crucible system.

Pelleted powders are unsatisfactory, since the fluoride is harder than the metal pellet presses, and impurities are introduced by slow drying of wet precipitated AmF_3 or by hydrofluorination of dried $Am(OH)_3$. The use of $Am(OH)_3$ is less convenient, does not always yield chunks, and is prone to losses. The wet precipitated AmF_3 has the disadvantage that small amounts of oxygen may be incorporated in the final fluoride in the form of oxyfluoride.

Care must be taken to dry the fluoride carefully; otherwise, when used in a reduction, the product will be americium monoxide. If the fluoride is not stored in a desiccator, it apparently picks up enough water to yield monoxide on subsequent reduction. Several fluoride preparations gave good metal when first prepared but gave americium monoxide after standing in air for 2 to 3 weeks. In this work both "dry" and "wet" prepared americium trifluoride have been used, yielding similar metal. The most successful procedure has been to precipitate the fluoride with hydrofluoric acid; wash with water (if washed more than two or three times the fluoride invariable peptizes, making quantitative recovery difficult); centrifuge repeatedly, drawing off the supernatant; dry in a vacuum desiccator over anhydrous phosphorous pentoxide; and dry at 200 to 400°C on the reduction apparatus before firing.

3. Type of Crucible System

Ideally, the crucible system should fulfill the following requirements:

(a) be unreactive,

(b) yield reproducible effusion conditions,

(c) keep solid reductant metal from contacting the fluoride,

(d) be easy to load,

(f) permit easy removal of the product.

As mentioned in the introduction, double crucible systems made either from refractory oxides or tantalum have been used successfully in metal preparation. Refractory oxide systems have the disadvantage that they must be fired at 1600 to 1800°C for several hours in order to harden and degas them. The effusion orifice is not reproducible, and it is difficult to estimate the rate of effusion of the excess reductant and consequently the reduction time. The porosity of the refractory inner crucible is variable. In many reductions carried out in these systems the americium metal soaked into the crucible, making recovery of the product impossible. As a result of these difficulties, tantalum has been used in the majority of the reductions for the crucible system.

Tantalum has the disadvantage that it is wet by americium at 1050 to 1100°C. When solid tantalum inner crucibles were used in reductions made above about 1100°C, the product spread and recovery was impossible. As reduction temperatures of 1100°C have proved the most successful, the inner crucible has been made in the form of a basket of 3-mil tantalum wire in order to minimize the tantalum surface exposed. The final form of the crucible system is sketched in Fig. 1. The basket holds the fluoride securely. In the event that the americium wets the basket, the tantalum can easily be cut away from the product with a loss of only 10 to 20% of the americium. In most of the measurements made on the metal, the presence of tantalum was not a disadvantage; in the melting-point determination and high-temperature x-ray studies, it was a definite advantage.

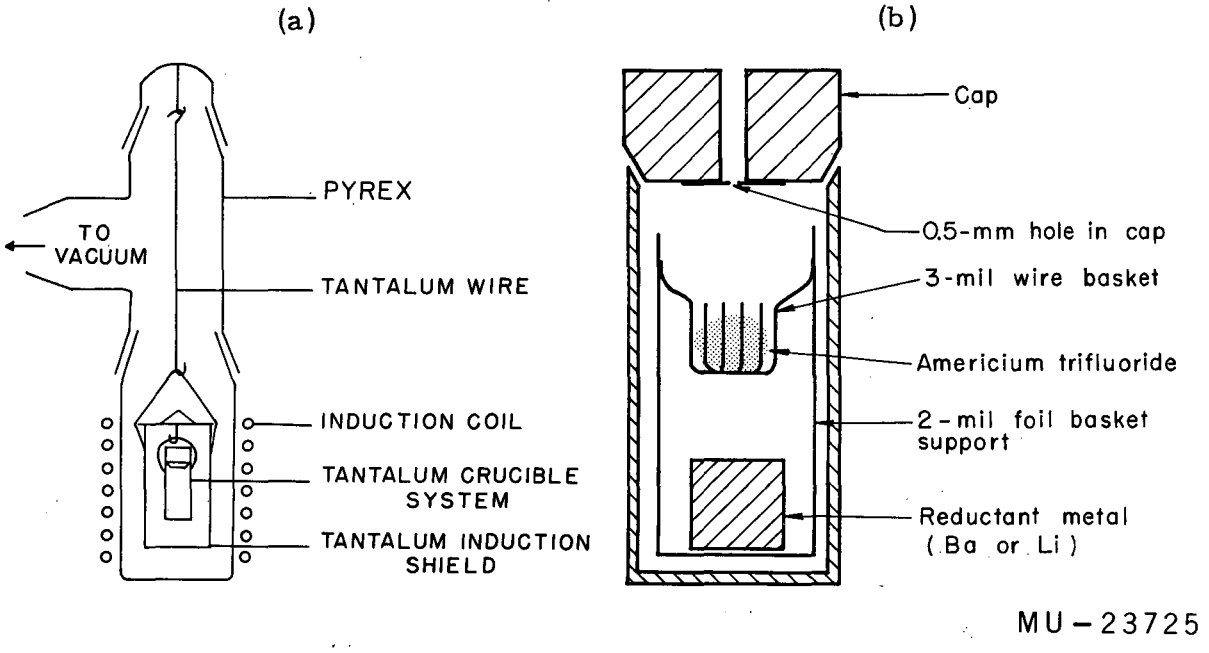

Fig. 1. Apparatus for the reduction of AmF_3 with Ba.
a. Microscale metal-production apparatus.
b. Crucible (all-tantalum components).

The inner crucible assembly could be loaded quickly and easily, thus cutting to a minimum the exposure of the fluoride and reductant metal to the nitrogen atomosphere of the box. (The "dry" box, even when flushed with dried nitrogen, is not free of oxygen and water because of diffusion through the gloves, and speed is essential.) The size of the hole drilled in the cap of the crucible can be adjusted to fit the desired duration of reduction at the chosen reduction temperature. The rate of effusion from a crucible can be estimated for Knudsen conditions by the equation

$$R(\text{moles/min/mm}^2) = 3.5\times10^{-2}\, p_{mm}/\sqrt{MT}\,, \qquad (1)$$

where

R is the rate of effusion of a gas from the orifice in moles per minute per mm^2 of orifice area,

p is the vapor pressure of the americium or barium,

M is the molecular weight,

T is the absolute temperature.

(As the system does not match ideal conditions for Knudsen effusion, the actual effusion will be slower than the above estimate.) An effusion hole of approximately 0.5 mm diameter is convenient for most reductions.

Tantalum cannot be degassed completely below approximately 2400°C, but is a "getter" for oxygen and nitrogen at 1000°C and helps to prevent reaction with residual gases.[17] The inner tantalum crucible usually is destroyed in removing the product, but the outer crucible system may be recovered by cleaning it in 6 M nitric acid and heating to 1000 to 1200°C for 20 to 30 min. It can be used for half-a-dozen reductions without noticeable contamination of the product resulting from degassing of the system.

4. Reduction Temperature and Duration of Reduction

The reduction temperature is critical. If it is too low, the resulting metal is impure; if it is too high, the metal vaporizes. Reductions carried out below the melting point of americium (995°C) typically contain 5 to 20 mole % barium. Between the M.P. and approximately 1100°C, the product is still surrounded by the barium fluoride slag, which apparently inhibits the vaporization of the excess barium, and, even with reduction times as long as 20 minutes, the products contain 2 to 5 mole % barium. Above 1100°C the metal wets the tantalum, leaving part of the metal exposed, and products with as little as 0.2 mole % barium have been obtained.

The reduction time is dependent on the temperature, size of crucible orifice, and amount and nature of excess reductant. A significant amount of time is needed for the crucible system to reach the reduction temperature. This can be reduced by initially setting the heater to a kilovolt reading corresponding to a much higher equilibrium temperature and then cutting back to the desired temperature. In a typical reduction 5 mg of americium trifluoride (17 micromoles of Am) are loaded with a tenfold excess of barium (200 micromoles). With a 0.5-mm-diameter orifice and a reduction temperature of 1100°C, it can be estimated from Eq. (1) that the barium will effuse at a rate of approximately 320 μM/minute and the americium at 0.1μM/min. The induction heater is set to a kv reading corresponding to 1300°C until the barium starts to effuse (40 sec). Then the temperature is dropped to 1100°C for 2.5 min, after which the sample is annealed. By use of these conditions, metal with 0.3 mole % detectable cationic impurities has been obtained.

5. Effect of Annealing and Cooling Rate

Unlike neptunium and plutonium, americium must be annealed to give well crystallized metal. In reductions made above the melting point of americium in which the product was not annealed but cooled to room temperature in vacuum, the metal was very poorly crystallized. The x-ray diffraction patterns showed only a few (6 to 12) weak lines which could be indexed as an hexagonal close-packed (hcp) structure. However, with the exception of the 10.1 reflection, most of the lines are coincident with those of a face-centered cubic (fcc) structure. Similar phenomena have been seen in cobalt and have been attributed to stacking faults in the hexagonal layers that make up both structures.[18] The problem of stacking faults of this type has been treated by Wilson,[19] who has shown that hexagonal reflections with (h-k)/3 integral and ℓ even will superimpose on the cubic reflections and be sharp. The remaining lines will be broadened because of the stacking faults. The unannealed americium metal is probably best described as a random stacking of hexagonal layers to form small crystallites.

Metal that was annealed (either during initial preparation or on reheating) for 4-hour periods at temperatures ranging from 750°C to 900°C and cooled to room temperature at the rate of 1.5 to 2°C/min gave much stronger x-ray diffraction patterns. The lines index as double hexagonal close-packed (dhcp), but there are still stacking faults, as evidenced by the line intensities (I(hk.l)). For a dhcp structure, I(00.4) < I(10.2). As stacking faults appear, the ratio of I(00.4)/I(10.2) appears to decrease because of the broadening of the 10.2 reflection. No fcc reflections that do not superimpose on dhcp reflections are visible, but the dhcp reflections that do superimpose on fcc reflections appear to be stronger than would be calculated for a dhcp structure.

Reductions carried out at approx 1000°C and cooled in vacuum for 5 to 10 hours yield x-ray diffraction patterns which agree very well with the intensities calculated for a dhcp structure. These patterns are the only ones for which, from visual estimates, I(00.4) < I(10.2).

In none of the initial preparations mentioned above are the high-angle diffraction lines sharp enough to show separation of the CuK_a doublet. This observation indicates that the individual crystals are very small. However, metal samples sealed in 1/3 atm of dry argon and heated in quartz capillaries showed a sharpening of the high-angle lines between 300 and 400°C. The stacking faults remained, but there was good separation of CuK_{a_1} and CuK_{a_2}.

At 400 to 500°C lines corresponding to americium monoxide (fcc, a = 5.05 A) sometimes appeared. The two phenomena seem to be independent, but this does not eliminate the possibility of oxygen or nitrogen stabilization of the metal phase.

On the basis of these experiments, it is concluded that americium must be annealed in order to eliminate a high proportion of stacking faults. It should be annealed as close to the melting point as possible. To obtain larger crystals the metal should be annealed between 300 and 500°C for periods of 24 to 48 hours.

6. Method of Heating

Three methods of heating have been used, with varying degrees of success:

(a) electron bombardment,

(b) resistance heating,

(c) induction heating.

The choice among them is mainly one of convenience and reproducibility. Electron bombardment is the most efficient, but the measurement of the temperature with an optical pyrometer is uncertain because of the reflection from the filament and the emissivity correction that has to be made. Far more important is the difficulty in controlling the temperature because of the arcing that occurs when the excess barium effuses from the crucible.

Resistance heating is inefficient, but it provides good temperature control from the reduction temperature to room temperature. As with electron bombardment, the effusion of the excess barium can be followed by its green glow. This method has two disadvantages. First, the coil is fragile, and second, the tantalum crucible has to be insulated from the heater. A thoria liner has been used as an insulator, but this requires extensive degassing.

Although resistance heating has been used successfully in many reductions, the author prefers induction heating. It provides accurate temperature control and permits accurate temperature measurement and is easy to use. The induction apparatus is sketched in Fig. 1. In a typical experiment, the blank crucible system is assembled and heated to 1000°C to vaporize the copper resulting from spot-welding the tantalum assembly. The copper condenses on the walls of the vacuum system and would lead to an error in the measurement of the temperature if not removed before the calibration. A clean pyrex bulb is put on the line, and the temperature of the crucible system, as measured through a hole in the induction shield with an optical pyrometer, is calibrated against the kilovolt setting on the power supply. The fluoride and barium are then loaded, and the reduction is carried out as described above. The whole operation can easily be accomplished in a day and is therefore much faster than either of the other methods.

As extensive compilation of experimental data, illustrating the effect of the variables discussed in the preceding sections of this thesis, is presented in Table III.

Table III. Summary of the pertinant americium metal preparations

No.	Reductant	T (°C)	Time (min)	Anneal (°C)	Cooling	Inner cruc.	Heating	At % red.	X-ray	Comments
1	Li	900	15	none	in vac.	Ta	I	10	M-dhcp +fcc Am0	Metal had black coating
2	Li	900	20	none	in vac.	Ta	I	9.5	M-dhcp + fcc Am0	Two pieces of metal with black coating
3	Li	900	25	none	in vac.	ThO_2	I	-	M-dhcp + fcc Am0	Two pieces- shiny on scraping, malleable
4	Li	1000	10	none	in vac.	ThO_2	I	-	-	Product soaked in and not recovered
5	Li	1015	6	none	in vac.	Ta	I	-	M-dhcp	Good metal
6	Ba	1000	30	none	1°/min 825-500°	ThO_2	I	-	W-dhcp	One piece of metal, 4 pieces of brittle material
7	Ba	1175	5	none	in vac.	ThO_2	I	-	-	Product soaked in
8	Ba	978	30	none	in vac.	Ta	I	-	VG-dhcp	Four pieces of metal surrounded by slag
9	Ba	995	30	none	in vac.	Ta	I	2.8	VG-dhcp	One chunk metal surrounded by slag
10	Ba	1010	30	none	2.5°/min 900-200°	Ta	I	-	VG-dhcp	Three pieces of good metal
11	Ba	1020	10	none	in vac.	Ta	I	-	M-dhcp + fcc (Am0)	One piece of metal surrounded by slag
12	Ba	1027	8	none	in vac.	Ta	I	3.7	-	Single large piece surrounded by slag
13	Ba	1015	10	non	in vac.	Ta	I	9	M-dhcp	Single large piece surrounded by slag
14	Ba	1037	6	none	in vac.	Ta	I	-	M-dhcp	Ball of metal
15	Ba	1000	30	none	in vac.	Ta	I	9	G-dhcp	Single piece covered with slag
	Ba	1016	10	none	in vac.	Ta	I	5	G-dhcp	Sample reheated with Ba
16	Ba	1300 1082	0.5 10	none	in vac.	Ta foil	I	-	-	Product spread
17	Ba	1300	0.5	none	in vac.	Ta basket	E.B.	10	M-dhcp	Current constant; T lower during effusion of Ba
18	Ba	1300	0.5	none	in vac.	Ta-B	E. B.	-	-	Product vaporized; piece of slag in crucible
19	Ba	1300 1130	0.5 3	none	1.5°/min	Ta-B	R	0.1	G-dhcp +bcc(Ta)	ThO_2 cap; product wet basket
20	Ba	1300 1130	0.5 3	4 hr 800	1.5°/min	Ta-B	R	-	P-dhcp +bcc(Ta)	ThO_2 cap; Ba not all vaporized; product spongy
21	Ba	1300 1130	0.5 3	1 hr. 900 1 hr. 850 1 hr. 800 5 hr. 500	1.5°/min	Ta-B	R	2.5	G-dhcp	ThO_2 cap; product wet basket; current held down during reduction
	Ba	1130	3	30 min 800	in vac.	Ta-B	R	0.8	M-dhcp + fcc Am0	Reheated to remove Ba
22	Ba	1300 1130	0.5 3	4 hr. 800	1.5°/min	Ta-B	R	1.2	G-dhcp	ThO_2 cap; product wet basket
				4 hr. 900	1.5°/min	Ta-B	R	-	No change in dhcp+fcc(Am0)	Product reannealed
				4 hr. 840	1.5°/min	Ta-B	R	-	No change	Product reannealed
				4 hr. 790	1.5°/min	Ta-B	R	-	No change	Product reannealed
23	Ba	1300 1130	0.5 4	4 hr. 850	1.5°/min	Ta-B	R	0.2	M-dhcp + bcc (Ta)	Product wet Ta, Tho_2 cap
24	Ba	1300 1130	0.7 4	4 hr. 775	1.5°/min	Ta-B	R	9	M-dhcp	Ta cap; 1/3 mm orifice; product surrounded by slag; Ba not all vaporized
		1300 1130	0.5 3	4 hr. 760	1.5°/min	Ta-B	R	9	M-dhcp	Product reheated without removing slag
25	Ba	1300 1130	0.5 5	3 hr. 800 1.5 hr. 700 4 hr. 500	1.5°/min	Ta-B	R	2.7	P-dhcp	Ta cap; 1/3 mm orifice; product wet basket
26	Ba	1300 1130	0.1 5	none	in vac.	Ta-B	I	6	P-dhcp	Ta cap; 1/2 mm orifice; induction system not reach reduction T in 5 sec
27	Ba	1300 1130	0.7 2.5	none	in vac.	Ta-B	I	0.2	P-dhcp	Ta cap; 1/2 mm orifice; 2/3 product vaporized; product, basket, slag all separate
28	Ba	1300 1130	0.8 2.5	none	in vac.	Ta-B6	I	0.1	P-dhcp	Ta cap; 1/3 mm orifice; product wet basket

Legend:

1. Amount of starting fluoride varies from 1 to 5 mg.
2. T dropped directly to annealing Temp. Cooling rate applies from annealing Temp. down to room temp.
3. Method of heating: I - Induction, E. B. - Electron Bombardment, R - Resistance.
4. X-ray: VG- Very good I(00.4) < I(10.2), G- good-some stacking faults, M- moderate- many faults but still dhcp, P- poorp 4 to 10 lines hcp.

B. Reduction of Americium Dioxide with Lanthanum Metal

In this method of americium metal preparation, 1- to 5-mg quantities of americium dioxide are reduced with lanthanum metal at 1200°C. The americium so produced is vaporized onto a quartz fiber or tantalum wire. This method has the advantage that the product is separated from the reaction mixture by vaporization and will be contaminated only by other volatile components of the system. In the fluoride reductions with barium, the sample must be separated mechanically from the slag and crucible system. The oxide-reduction apparatus used in this study has an additional advantage in that the product may be dropped directly into an x-ray capillary and sealed without breaking the vacuum. This diminishes the possibility of reaction with the air.

The estimated ΔF for several of the possible reactions indicates that they are thermodynamically favorable:[12]

$$AmO_2 + (4/3)\,La \rightleftharpoons Am + (2/3)La_2O_3, \quad \Delta F_{1500^\circ K} = -44 \text{ kcal};$$

$$AmO_2 + (1/3)La \rightleftharpoons (1/2)Am_2O_3 + La_2O_3, \quad \Delta F_{1500^\circ K} = -41 \text{ kcal};$$

$$(1/2)Am_2O_3 + La \rightleftharpoons (1/2)La_2O_3 + Am, \quad \Delta F_{1500^\circ K} = -3 \text{ kcal}.$$

The success of this technique depends on the relative volatility of americium and the other components of the system. The effusion equation (1) shows

$$R(\text{moles/min/mm}^2) \propto p_{mm}/\sqrt{M}.$$

From the vapor pressure equations of lanthanum[20] and americium,[2]

$$\log(R_{La}/R_{Am}) = -7{,}300/T + 1.06,$$

where T is the temperature in °K. However, lanthanum will also effuse as LaO. This results from reactions of the type

$$La_2O_3(s) \rightleftharpoons LaO(g) + \tfrac{1}{2}\,O_2(g)$$

and

$$La(\ell) + La_2O_3(s) \rightleftharpoons 3\,LaO(g)\,.$$

The ratio of the vapor pressures of LaO and La can be estimated for our reduction temperature from the work of Chupka et al.[75] ($p_{LaO}/p_{La} = 2.5$), and the total rate of effusion of lanthanum will be larger by a factor

$$\left[1 + \left(\frac{m_{La}}{m_{LaO}}\right)^{1/2} \frac{p_{LaO}}{p_{La}}\right] = 3.3 .$$

Therefore,

$$\log (R_{La(total)}/R_{Am}) \approx - 7,300/T + 1.58 .$$

The reduction temperature is chosen according to the desired rate of effusion of americium and the percent of lanthanum calculated from the equation above. (It should be noted that the effusion of LaO means that not only lanthanum but also oxygen is in the product metal.) A satisfactory rate of 2.4 μM/min is calculated for pure americium metal at 1200°C with a 20-mil hole in the crucible cap. However, the americium is dissolved in molten lanthanum, and its vapor pressure undoubtedly is somewhat less than calculated.

The apparatus is sketched in Fig. 2. The inner crucible has a tapered bottom so that the reactants will maintain maximum contact. Reductions made with a flat-bottomed crucible often yielded little or no coating on the fiber. The vertical position of the crucible system can be varied by putting spacers in the crucible holder. A fiber-to-crucible distance of 1 to 2 mm is convenient. (Allowance must be made for the thermal expansion of the tantalum crucible; otherwise, the crucible and fiber may make contact at high temperatures, ruining the experiment.) Either a 10-mil tantalum wire or quartz fiber may be placed in the chuck as shown. The chuck can then be rotated and moved horizontally by magnets. After a satisfactory deposit is obtained, the apparatus is rotated 90 deg, and the fiber assembly is lowered into the capillary. The fiber, after being released by lifting the clamp with a magnet, falls into an x-ray capillary which is then sealed off.

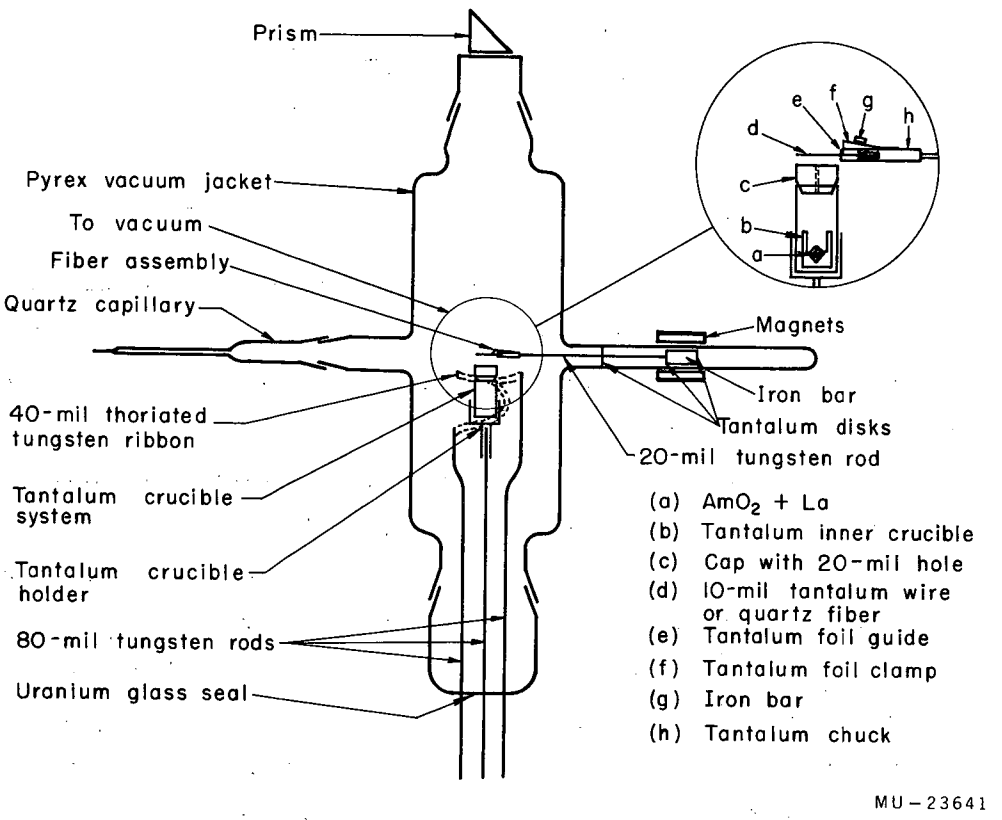

Fig. 2. Apparatus for reducing americium dioxide with lanthanum metal.

The americium dioxide is made by precipitating the oxalate and igniting it in air at 600°C. The ignition temperature evidently should not exceed 600°C by much, since it was found that when the oxalate was ignited at 800 to 900°C, reductions using the resulting oxide did not yield coatings even after 30 to 40 minutes at 1200°C.

In a typical experiment a fiber or wire is cleaned in nitric acid, water, and carbon tetrachloride, and is loaded. A piece of lanthanum is put in the inner crucible and the line assembled. The crucible is heated to 1200°C for 2 minutes to melt the lanthanum, causing it to spread as a layer of lanthanum on the bottom of the crucible. Several additional pieces of lanthanum are scraped clean and loaded into the inner crucible along with an approximately stoichiometric amount of americium dioxide, and the system pumped down to a pressure of 2 to 4×10^{-7} mm. The tip of the fiber is pushed over the hole in the crucible. The crucible system is heated to 1200°C for 30 min, and the fiber is rotated 90 deg every 3 to 4 min. The fiber is then dropped into the capillary and sealed off.

The method and apparatus were tested with samarium, dysprosium, and erbium sesquioxides. In each case shiny metallic coatings were obtained. The crystal structure and lattice parameters of each of the coatings were in agreement with the published data on the respective metals. Although the structure of samarium involves a rather complicated sequence of nine hexagonal close-packed layers in the unit cell,[21] it nevertheless was reproduced under these conditions in which the vapor is condensed on a fiber at a temperature of 100 to 300°C. In the erbium sesquioxide reductions a temperature of 1400°C and effusion time of 25 min yielded metal with 5 wt % lanthanum, while with a temperature of 1530°C and time of 4 min lanthanum was present to the extent of 10 wt %. This indicates that the reduction temperature should be kept as low as possible.

With americium dioxide shiny metallic coatings of approximately 100 μg of americium were collected. Spectrographic analysis typically

showed 1 at.% lanthanum. The x-ray patterns were predominantly fcc with a few hcp lines (also occasionally americium monoxide lines). The fcc structure was evidently quenched to room temperature by this method of collection. Coatings have been collected both on quartz fibers and on tantalum wires with no apparent difference in the products. To minimize the possibility that the condensed phase was impurity-stabilized, a sample of bulk metal made by a fluoride reduction was vaporized and collected on a tantalum wire. The x-ray diffraction pattern was similar to those obtained in the oxide reductions.

C. Americium Monoxide

Americium monoxide was first reported by Zachariasen as a phase observed in an attempted preparation of americium dichloride ($AmCl_2$) by Fried.[22] It was reported as being fcc with a = 4.96 A. In several attempted preparations of americium metal in this Laboratory--principally by Cunningham and Wallmann--using "wet" precipitated fluoride a metallic-looking but brittle product was obtained. This material yielded sharp, strong x-ray diffraction lines which were indexed as fcc with a = 5.053 A. It was suspected that this material was americium monoxide. The lattice parameter differed greatly from that reported by Zachariasen, but his product was stated to be of unknown purity. Several attempted oxide reductions in which the experiment was not done carefully showed varying amounts of americium monoxide and americium metal by x-ray diffraction. One coating on tantalum gave an x-ray pattern showing predominantly a fcc structure with a = 5.054 A (the other lines were tantalum lines and three lines which coincided with those of fcc americium metal.) Another coating on quartz gave a lattice constant of a = 5.053 ± .004 A.

Akimoto has prepared a sample of bulk phase americium monoxide by reacting americium metal with a stoichiometric amount of oxygen in a quartz tube at 800°C. The x-ray pattern was indexed as fcc with a = 5.048 A.[23]

In a high-temperature x-ray study of americium metal at temperatures up to 850°C, the metal reacted with the walls of the capillary, and the resulting material was fcc, a = 5.035 A at 20°C. Pictures taken at 210, 405, and 605°C gave lattice constants of 5.045 ±.002, 5.057 ±.003, and 5.070 ±.002 A respectively. The lattice constants of this sample are decidedly lower than the others reported above, indicating that the material is probably a mixture of americium monoxide and mononitride, as americium mononitride is also fcc with a = 5.000 A.[23]

The apparent reproducibility of this phase from many sources is evidence for a nearly constant composition. The preparation on tantalum with bulk oxide present is evidence for the phase's being an oxide and indicates a fairly stable material. This is further supported by the stability of the phase in high-temperature studies. The preparation of a bulk phase even when in contact with quartz suggests that the material is americium monoxide and that it may be stable at room temperature. It is evident, however, that a thorough study of the americium-oxygen system is needed to establish the actual composition and thermodynamic stability of americium monoxide.

D. Attempted Preparation of "Expanded" dhcp Americium Metal

Graf et al.[4] have reported that americium metal is dhcp with a = 3.642 ±.005 A and c = 11.76 ±.01A, giving a density of 11.87 ±.05 g/cm^3. Also, it was reported that between 400 and 600°C americium metal was fcc with a = 5.10 A at 600°C.[24] In the work presented herein, in some 40 successful metal preparations using both oxide and fluoride reductions, no metal with the larger lattice constants has been obtained. All of our successful reductions show only the fcc or dhcp structures reported in the section on crystal structure.

The reduction conditions used by Graf have been duplicated as closely as possible. From his notebook and from what his associates in this Laboratory remember, Graf's experimental technique was as follows: The americium trifluoride was prepared by wet precipitation

with hydrofluoric acid from a stock solution containing 1.4 mole cationic impurities according to spectrographic analysis. The fluoride was dried in the original plastic container in a vacuum desiccator over P_2O_5. The barium was from the same stock used in this study. A tantalum double crucible system with a thoria cap was used. The system was heated by resistance heating, and the crucible was insulated from the coil by a thoria liner. The fluoride was reduced at 1300°C for 30 seconds and 1130°C for 3 min. The product was then annealed at 800°C for 4 hours and cooled at a rate of 1.5 to 2°/min to room temperature. Graf made seven reductions: five with Am^{241} and three with Am^{243}, using the same technique in all reductions. Spectrographic analysis on some of the products showed from 5 to 0.1 % cationic impurities. Six of the seven yielded the expanded dhcp structure. The x-ray patterns varied from moderate to poor and showed only broad high-angle lines. The other reduction yielded a poor pattern with 19 measureable reflections, 16 of which index as dhcp with a = 3.43 A and c = 11.14 A. The pattern is poor, but it definitely indicates the same structure that has been observed in this study.

The high-temperature x-ray studies made by Graf show no measurable lines up to 400°C. The fcc structure seen between 400 and 600°C has a lattice constant very similar to that of americium monoxide. The appearance of this phase at approximately 400°C is in agreement with the results obtained in this study. Above 600°C a complex pattern appeared which is similar to that expected for higher oxides of americium. It seems that the high-temperature phase reported by Graf was americium monoxide.

As discussed in the section on fluoride reductions, metal preparations have been made in this work by using resistance heating, thoria liners, thoria crucible caps, and annealing conditions similar to Graf's (see Samples 19 through 25 in Table III). The author has been unable to reproduce or account for the formation of the "expanded" dhcp phase. It is possible that small amounts of anionic impurities

such as hydrogen, carbon, or nitrogen might cause an expansion of the lattice. For example, the formation of americium mononitride and americium monoxide results in lattice expansion. Another argument that supports the possibility of an interstitial compound is that the metallic radius for the "expanded" structure is 1.82 A. In a plot of metallic radius against atomic number for the actinide metals this point lies above the curve connecting actinium and curium (see Fig. 18), which would indicate fewer than three conduction electrons. At present the "expanded" dhcp phase remains a mystery.

E. Purity of Americium Metal Samples

The spectrographic results for the samples used in the measurements discussed in Sections II, III, IV, and V are listed in Table IV. The sample numbers correspond to reductions in Table III. All quantities are in micrograms. The blanks have been corrected to a volume equivalent to the sample volume. The impurities detected are listed in the top of the table, and the limits of detection of other elements are listed in the bottom of the table.

Table IV. Purity of the americium metal samples.

Sample		Am	Al	Ba	Ca	Mg	Total mole % Am
28	sample	50.4	<0.01	0.04	0.01	<0.01	
	blank	-	<0.01	-	0.003	<0.01	
	mole %	-	-	0.12	0.08	-	99.80
27	sample	48.4	0.07	0.05	<0.01	<0.01	
	blank	-	<0.01	-	<0.01	<0.01	
	mole %	-	1.32	0.18	-	-	98.50
25	sample	63.9	0.02	1.0	0.02	<0.01	
	blank	-	<0.01	-	0.01	<0.01	
	mole %	-	0.27	2.74	0.12	-	96.87
23	sample	73.8	<0.05	0.1	0.02	<0.01	
	blank	-	<0.01	-	0.01	<0.01	
	mole %	-	-	0.18	0.07	-	99.75
22	sample	30.6	0.02	0.2	0.01	0.01	
	blank	-	0.005	-	0.005	0.005	
	mole %	-	0.45	1.45	0.10	0.16	98.13
19	sample	47.2	0.02	0.03	0.02	0.01	
	blank	-	0.01	-	0.005	0.01	
	mole %	-	0.38	0.11	0.19	0.21	99.11
17	sample	40.0	0.02	2.0	0.02	0.01	
	blank	-	<0.01	-	0.01	<0.01	
	mole %	-	0.45	8.8	0.15	0.25	90.4
13	sample	39.2	0.02	2.0	0.1	0.05	
	blank	-	0.015	-	0.015	<0.005	
	mole %	-	0.34	9.0	1.31	1.14	88.21
9	sample	31.5	0.05	0.5	0.05	0.03	
	blank	-	<0.01	-	0.005	0.005	
	mole %	-	1.42	2.80	0.86	0.80	94.12

Limits of detection (μg) with Cu spark

Ag <0.01	Fe <0.01	Mo <0.01	Rh <0.1	Tl <0.1
As <0.05	Ga <0.1	Na < 1	Ru <0.1	Tm < 0.05
Au < 0.5	Gd <0.05	Nb < 0.01	Sb <0.5	U <0.1
Be <0.01	Ge <0.05	Nd <0.1	Sc <0.01	V <0.05
Bi <0.05	Hf <0.1	Ni <0.05	Si <0.01	W <0.1
Cd < 0.5	Ho <0.05	Np < 1	Sm <0.05	Yb <0.01
Ce <0.1	In <0.05	Os <0.1	Sn <0.1	Y <0.01
Cm < 1	Ir <0.5	Pb <0.1	Sr <0.01	Zn <0.1
Co < 0.05	K < 1	Pd <0.1	Ta <0.1	Zr <0.01
Cr <0.01	La <0.01	Pr < 1	Tb <0.1	
Dy <0.05	Li < 1	Pt <0.1	Te <5	
Er <0.05	Lu <0.05	Pu< 1	Th <0.5	
Eu <0.01	Mn <0.01	Re <0.1	Ti <0.01	

III. MELTING POINT OF AMERICIUM METAL

There was a large uncertainty in the melting point of americium metal. Westrum and Eyring[1] reported that there was a softening of the metal at 850°C, but even at 1200°C melting seemed incomplete. Several other attempts have been made in this Laboratory to determine the melting point of americium.[24] In most cases the metal deformed slightly between 825 and 850°C but no further change was seen. In all these experiments the melting point apparatus consisted either of a tantalum hairpin with metal between the jaws or of an anvil and plunger assembly separated by metal. The melting point was taken as the temperature at which the jaws closed or the plunger dropped. At elevated temperatures a coating of oxide or nitride often forms around the metal and supports the hairpin or plunger to temperatures well above the melting point of the metal, leading to an erroneous or uncertain result.

The preparation of americium metal by the reduction of the fluoride in a tantalum wire basket produces a sample of metal in a form convenient for determination of the melting point without the uncertainties resulting from surface coatings. As the americium metal wets the tantalum, a set of tantalum wires essentially soldered together by americium is obtained. To determine the melting point, the sample is suspended from one wire and a weight is hung on the other. At the melting point the wires separate and the weight falls. This method has the advantage that there is a metal-to-metal bond, and no oxide or nitride coating can form between the metals. As americium does not appear to alloy with tantalum, the observed melting point is that of pure americium metal.

The apparatus is sketched in Fig. 3. The temperature of the inner radiation shield is measured with an optical pyrometer, and the temperature is calibrated by using gold, cerium, and praseodymium [a Ta-(Ce or Pr)-Ta assembly similar to that for americium was used in the calibration]. The melting point is observed by the dropping of the tantalum vane. After a run both wires had americium metal on them,

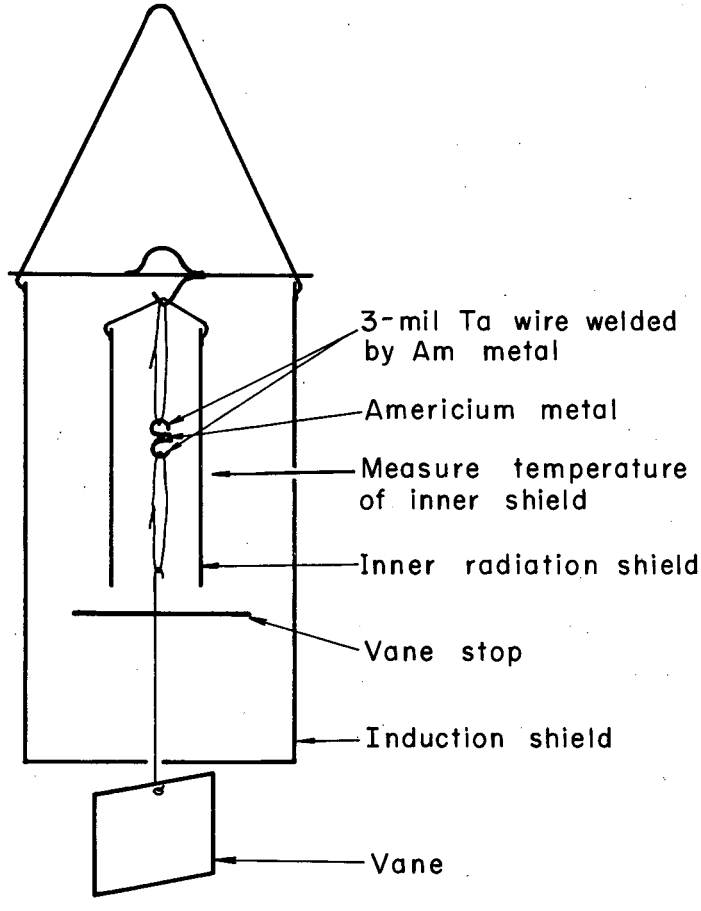

Fig. 3. Melting-point apparatus.

Table V. Melting point of americium metal

Sample	Run	$T_{observed}$ (°C)	ΔT[a]	T_{mp} (°C)
22	1	994 ± 16	-	994 ± 16
	2	1006 ± 2	-9 ± 2	997 ± 4
23	1	1003 ± 2	-9 ± 2	994 ± 4
Average:				995 ± 4

[a]Determination of ΔT

Sample	T_{mp} (°C)	T_{obs} (°C)	T
Au	1063	1073	-10
Pr	935	942	- 7
Ce	804	811	- 7

(Sample 22, Run 1 did not have an inner radiation shield and the actual wire was observed.)

indicating that the metal had melted and that a Ta-Am joint had not broken. An x-ray pattern taken after a run showed lines corresponding to americium metal, tantalum, and americium monoxide. The results of three independent determinations are listed in Table V, and the average gives a melting point of 995 ± 4°C.

IV. CRYSTAL STRUCTURE OF AMERICIUM METAL

A. Experimental Procedure

In the past the experimental techniques for obtaining x-ray diffraction patterns from actinide elements and compounds have differed only slightly from standard methods although the preparative techniques were often unique. The major change in the x-ray work was that the samples were mounted in thin-walled pyrex or quartz capillaries.[26] As crystal structure studies progress to higher members of the actinide series, the samples become smaller, more valuable, and more radioactive, and it is desirable to have an x-ray powder camera that combines the following properties:

- capable of conveniently covering a reasonable range of temperatures and having the usual desirable features of high- and low-temperature cameras as discussed by Goldschmidt and Steward;[27]
- having vertical suspension to prevent the sample from rolling out of the beam, and microadjustment of the capillary to insure optimum exposure;
- capable of accommodating a long capillary, thus allowing it to be broken and resealed several times to perform chemical reactions without having to transfer submicrogram samples;
- having interchangeable collimators for varying sample sizes;
- minimizing handling of fragile capillaries to provide maximum safety;
- capable of taking several exposures without disturbing the adjustment of the capillary.

These properties were realized by constructing a camera similar to the high-temperature camera designed by Buerger et al.,[28] except that the whole camera was rotated 90 deg around the x-ray beam axis. The general design of the camera is shown in Fig. 4. The camera diameter is 90 mm, a dimension chosen mainly to facilitate comparison with the film file in this Laboratory. The film is mounted

in a removable, full-circular cassette using a Straumanis-type film mounting. The film is pressed against the cassette by "claws." The x-ray gap in the cassette cover has a strip of 1/3-mil nickel foil to cut down background radiation, to make the cassette lighttight and to remove the copper K_β x-rays. Two sets of knife edges for calibration are machined in the cassette cover. The collimator consists of a double pinhole and scatter guard system similar to those used in the commercial Norelco powder cameras and discussed by Parrish and Cisney.[29] The base is designed to fit on a standard Norelco stand, and the capillary rotation mechanism is connected by an O ring to the motor in the stand. The chuck holder is interchangeable with an oven for high-temperature studies and is easily modified to take pictures below room temperature. The capillary assembly is held in the chuck by a screw and can be adjusted in three directions, as shown. The capillary assemblies used are shown in the inset in Fig. 4.

The oven contains a small, low-heat-capacity furnace consisting of a platinum wire coil wrapped on a ceramic form (Lava A is a very convenient material, as it can be machined and then fired). The oven has an 1/8-in. hole for the capillary and a central x-ray gap. The outside of the oven is water-cooled, and, as a radiological safety precaution at temperatures above 600°C, the x-ray gap is covered with 0.1-mil Mylar. The power is supplied by a step-down transformer controlled by a variac fed from a Sola constant-voltage transformer. The temperature is measured with a Pt; Pt, 10% Rh thermocouple and was continuously monitored by a Brown Recording Potentiometer. The thermocouple and the input current were calibrated against the melting points of standard substances sealed in quartz capillary assemblies. Diffraction patterns have been obtained at temperatures up to 850°C, but this is not an upper limit for the oven. The temperature control and measurement with the original oven was good within ± 5° up to 600°C. A second oven used between 800 and 850°C was calibrated to ± 15° with an optical pyrometer.

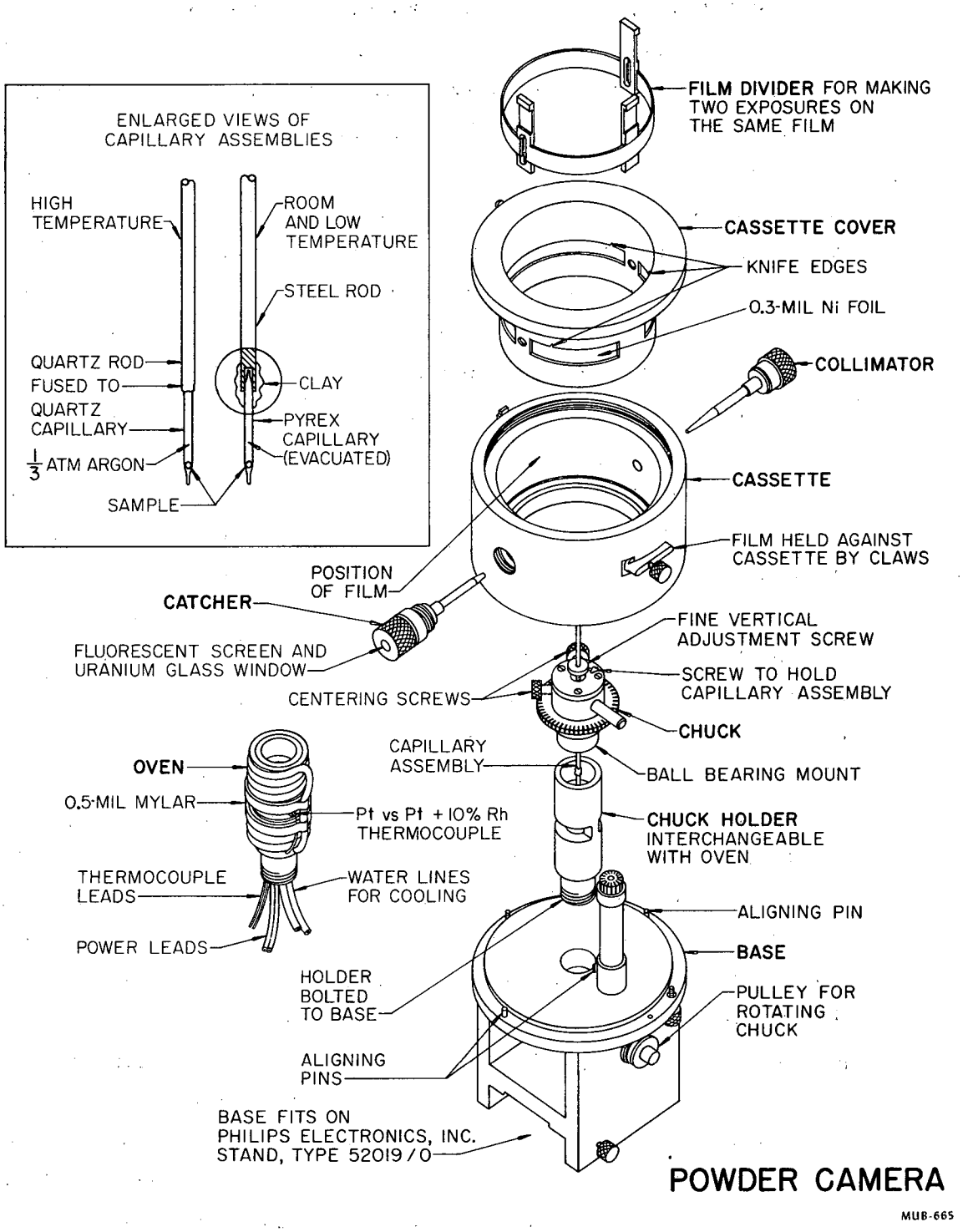

Fig. 4. X-ray powder camera.

The camera was modified to take diffraction patterns below room temperature, as shown in Fig. 5. A stream of dry nitrogen cooled by passing through liquid nitrogen was blown over the capillary. The temperature was controlled by varying the flow of nitrogen and was measured with a chromel-alumel thermocouple placed directly below the capillary. The top of the camera was sealed, providing a "dead air" space which reduces icing of the capillary and partially insulates the film. Temperatures of -125 ± 10^{6}C have been obtained. Below this temperature the chuck bearing froze. A cryostat could be made to fit the camera for obtaining lower temperatures, but was not needed in this study.

The camera described above provides a maximum of safety against breaking the capillary and contaminating the camera. In loading a sample, the capillary is checked for external alpha contamination in a box equipped with an alpha meter and fixed to the support rod with clay, thus completing the direct handling of the capillary. The camera is then put in the box, and the capillary assembly is loaded in the chuck. The chuck is placed in a stand and the sample is centered. The capillary is drawn up into the chuck which in turn is placed in the chuck holder. The capillary can now be lowered into position without danger of breaking it, and the final adjustment of the capillary can be made with the aid of a microscope. The cassette can be removed to change films without disturbing the capillary. The capillary adjustment screws, however, are exposed, and the capillary may be readjusted with respect to the x-ray beam as seen on the fluorescent screen.

Very little excess equipment is needed to obtain x-ray diffraction patterns on radioactive material. With a little care the samples can be sealed in an x-ray capillary in a "piano" box, and the capillary can be removed without contaminating the outside of the capillary. As described above, the capillary is loaded in the camera in a box. A lucite box fits over the top of the Norelco x-ray machine, and four sets of doors provide access to the x-ray ports. The box serves a twofold purpose: (a) if a capillary should break, it would provide a secondary

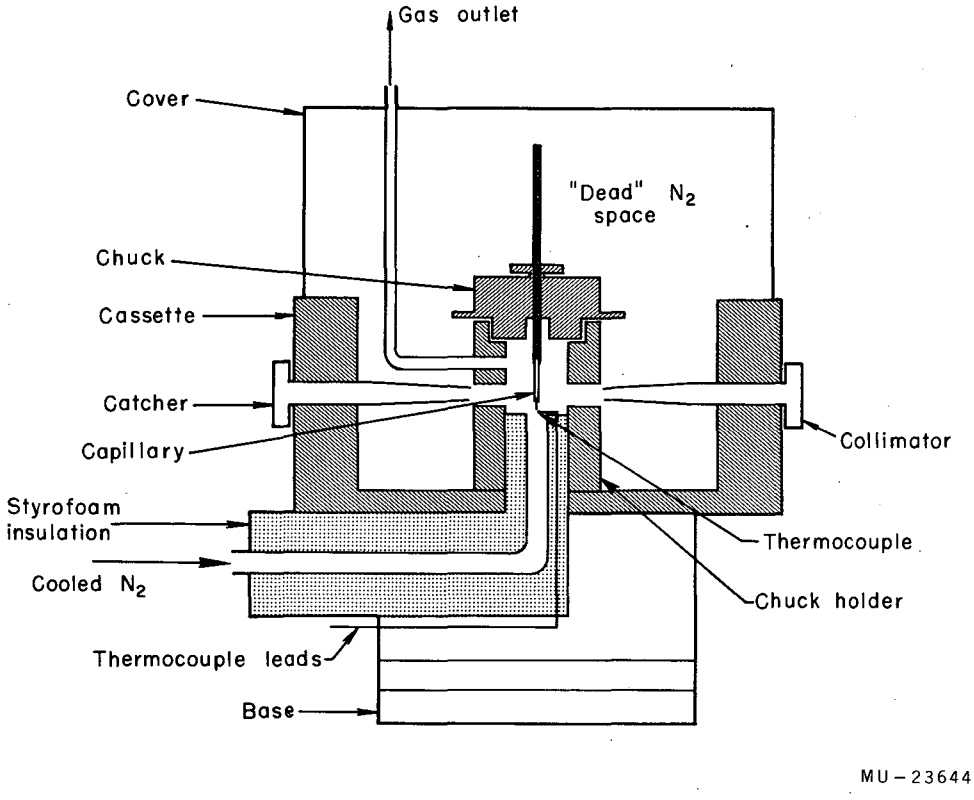

Fig. 5. Powder camera adapted for low-temperature measurements.

container for activity; (b) it stops the x-ray beam, and thus allows the camera to be aligned accurately with comparative safety. To do this the uranium glass window in the catcher is removed, and the beam intensity is measured with a "Juno" gamma meter, a far more sensitive test than visual observation of the fluorescent screen in the catcher.

It is necessary to use an x-ray film that provides a low background. Two types of film have been found convenient. Ilford "Industrial G" film is used for short exposures (3 to 8 hours) and Kodak AA film for long exposures (15 to 25 hours). The nickel foil placed between the sample and the film also helps to cut the background down.

A far more serious problem in this study is the reactive nature and volatility of americium metal. At elevated temperatures, the sample reacts with the walls of the quartz capillary, and at temperatures above approximately 600°C vaporizes onto the walls. By pre-degassing the capillary at 700 to 800°C and sealing the samples under a pressure of 1/3 to 1/2 atmosphere of argon, these problems were minimized. (The argon was purified by passing it through anhydrous magnesium perchlorate and then over calcium metal at 600°C). Up to about 600°C only minor reaction with the walls took place, as evidenced by four to eight x-ray diffraction lines of the fcc americium monoxide phase which usually appeared at about 400°C.

Several attempts were made to use americium-tantalum samples obtained from fluoride reductions and to mount the tantalum wires in quartz chucks in capillaries in order to prevent the americium from contacting the quartz, but no usable diffraction patterns were obtained. Instead, a short length of quartz rod was mounted in the capillary to act as a stand for the sample, as it was feared that the larger expansion of the metal relative to quartz might crack the capillary at high temperatures. The most successful capillary assembly for high-temperature studies was an all-quartz system of a quartz capillary used to a quartz rod. Attempts to seal the capillary to metal holder with Sauereisen (No. 7 insa-lute hi-temp cement) resulted in the capillary's cracking at high temperatures.

Because in several early attempts to determine the melting point of americium metal a deformation of the sample was observed between 825 °C and 850 °C, an attempt was made to obtain x-ray diffraction patterns at 850 °C. Even under 1 atmosphere of argon at 850 °C, the americium metal vaporized onto the capillary walls before a usable diffraction pattern could be obtained. To minimize the exposure time as much as possible without completely rebuilding the camera, a shorter film radius was obtained by wrapping the film directly around the oven. A film holder was made of black paper with nickel foil between the film and the oven to minimize heat transfer to the film. The camera diameter was approximately 38 mm, and diffraction patterns could be obtained in 30 to 40 minutes. Although the outer surface of the oven was not accurately round, the tantalum diffraction lines from the sample could be used as an internal standard.

B. Determination of Accurate Lattice Parameters

There are two types of errors to be considered in the determination of accurate lattice parameters. First, there are random errors associated with the measurement of an x-ray diffraction line on a film, and second, there are physical errors which change the positions of the lines on the film. These subjects are discussed in detail in many textbooks on crystallography, and will only be summarized here.[30, 31]

The major physical errors are: 1, film shrinkage; 2, sample eccentricity; 3, divergence and absorption of the x-ray beam.

1. Film shrinkage: In principle the Straumanis type of film mounting eliminates errors resulting from uniform film shrinkage, as it is self-calibrating. For any film, the average of the corresponding lines on each side of the beam entrance and exit holes gives the 180 deg and 0 deg points directly. Although it is obvious, very few textbooks emphasize that this is true only if there is no eccentricity in the sample axis. The discussions presented for eccentricity errors are usually based on symmetrical film mountings, and, therefore, the asymmetric mounting is discussed below.

2. Eccentricity: The effect of sample eccentricity perpendicular to the cylindrical axis of the film and to the x-ray beam is shown in Fig. 6. For small values of Δr, it can be assumed that $S_o \approx S$, and from the film X and Y can be determined. If $\Delta r = 0$, then θ (the Bragg angle = $(X_o/Y_o)90$, and there is no error in the measurement of θ due to eccentricity. However, for a small Δr, one has

$$X_o + \Delta S \approx X + \Delta r,$$
$$Y_o \approx Y + 2\Delta r,$$
$$\Delta S \approx (\Delta r \cot 2\theta)\sin 2\theta = \Delta r \cos 2\theta .$$

The equation for θ now becomes

$$\theta = (X + 2\Delta r \sin^2\theta)90/(Y + 2\Delta r).$$

If the camera has knife edges for calibration, then Y_o can be measured directly and Δr calculated. The equation for θ is simplified to

$$\theta = \theta_o + \Delta\theta_{ecc\perp}$$

$$\theta_o = \frac{X}{Y_o} 90, \quad \Delta\theta_{ecc\perp} = 90\left[1 - \frac{Y}{Y_o}\right]\sin^2\theta . \qquad (2)$$

The error in θ resulting from the sample's being displaced parallel to the beam will be the same as in cameras using symmetrical film mountings:

$$\Delta\theta_{ecc\parallel} \propto \sin 2\theta \qquad (3)$$

3. Divergence and absorption of the x-ray beam: It has been shown theoretically[32] and verified experimentally[33] that with a divergent x-ray beam from an exponential focus the error in θ resulting from absorption is:

$$\Delta\theta_{abs.} \propto \frac{1}{2}\left(\frac{\cos^2\theta}{\sin\theta} + \frac{\cos^2\theta}{\theta}\right). \qquad (4)$$

The error in the ideal Bragg angle can be treated as a correction term by expanding the expression for $\sin^2\theta$ as a Taylor's series.

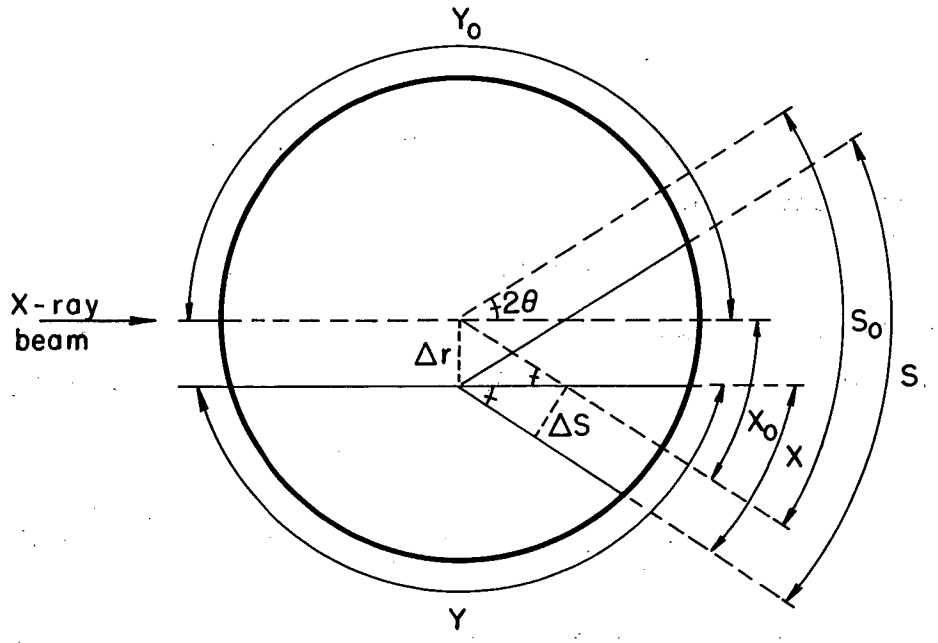

Fig. 6. Eccentricity error in a Straumanis film mounting.

In the hexagonal system we have

$$(h^2 + hk + k^2)A + \ell^2 C = \sin^2\theta + \Delta\theta \sin 2\theta + \cdots , \qquad (5)$$

where

$$\Delta\theta = D \sin 2\theta + E \left(\frac{\cos^2\theta}{\sin\theta} + \frac{\cos^2\theta}{\theta} \right) .$$

Equation (5) shows that the errors resulting from eccentricity, divergence, and absorption become zero at 90 deg. Cohen suggested using the method of least-squares to obtain the best fit for an equation such as (5), thus minimizing the random errors of line measurement and giving the best extrapolation function.[34] Hess indicated by a rather lengthy argument that in a least-squares treatment the lines should be weighted according to $w_i/\sin^2 2\theta_i$ for a Debye-Scherrer camera.

A much simpler argument to show the need for the factor $1/\sin^2 2\theta_i$ is as follows: the basic principle of least-squares is to minimize the weighted sum of the squares of the observed residuals, i. e.

$$S = \Sigma\, w_i(\theta_{i\ \mathrm{calc}} - \theta_{i\ \mathrm{obs}})^2 .$$

It is more convenient as shown above to treat an equation involving $(\sin^2\theta_{\mathrm{calc}} - \sin^2\theta_{\mathrm{obs}})$. However, this is not the observed variable, and from Eq. (5) one has

$$(\sin^2\theta_{\mathrm{calc}} - \sin^2\theta_{\mathrm{obs}}) \approx (\theta_{\mathrm{calc}} - \theta_{\mathrm{obs}}) \sin 2\theta_{\mathrm{obs}} .$$

The sum to be minimized is then

$$S = \Sigma\, \frac{w}{\sin^2 2\theta} (\sin^2\theta_{\mathrm{calc}} - \sin^2\theta_{\mathrm{obs}})^2 .$$

Using the definitions

$$\alpha_i = (h^2 + hk + k^2),$$

$$\gamma_i = \ell^2 ,$$

$$\delta_i = \sin^2 2\theta_i ,$$

$$\epsilon_i = \sin^2 2\theta_i \left[\frac{1}{\sin\theta_i} + \frac{1}{\theta_i} \right] ,$$

$$w_i = w_i / \sin^2 2\theta_i ,$$

$$V_i^o = A_o a_i + C_o \gamma_i - \sin^2 \theta_{i\,(obs)},$$

where A_o and C_o are approximate lattice parameters (D_o and E_o are set equal to zero as D and E are small), one can write

$$V_i = (A_o + \Delta A)a_i + (C_o + \Delta C)\gamma_i - \sin^2\theta_{i\,(obs)} + \Delta D\delta_i + \Delta E\epsilon_i .$$

Then in matrix notation the normal equations become

$$\begin{pmatrix} \Sigma a_i V_i^o w_i \\ \Sigma \gamma_i V_i^o w_i \\ \Sigma \delta_i V_i^o w_i \\ \Sigma \epsilon_i V_i^o w_i \end{pmatrix} = \begin{pmatrix} \Delta A \\ \Delta C \\ \Delta D \\ \Delta E \end{pmatrix} \begin{pmatrix} \Sigma a_i^2 w_i & \Sigma \gamma_i a_i w_i & \Sigma \delta_i a_i w_i & \Sigma \epsilon_i a_i w_i \\ \Sigma a_i \gamma_i w_i & \Sigma \gamma_i^2 w_i & \Sigma \delta_i \gamma_i w_i & \Sigma \epsilon_i \gamma_i w_i \\ \Sigma a_i \delta_i w_i & \Sigma \gamma_i \delta_i w_i & \Sigma \delta_i^2 w_i & \Sigma \epsilon_i \delta_i w_i \\ \Sigma a_i \epsilon_i w_i & \Sigma \gamma_i \epsilon_i w_i & \Sigma \delta_i \epsilon_i w_i & \Sigma \epsilon_i^2 w_i \end{pmatrix} ,$$

where each summation is over all N reflections. These are solved for $\Delta A, \Delta C, \Delta D,$ and $\Delta E,$ and the lattice parameters obtained from

$$a_o = \left(\frac{\lambda^2}{3(A_o + \Delta A)} \right)^{1/2} , \qquad C_o = \left(\frac{\lambda^2}{4(C_o + \Delta C)} \right)^{1/2} .$$

This problem has been programmed, using FORTRAN, for an IBM 704 computer by Mueller and Heaton at Argonne National Laboratory.[36, 37] Dr. Mueller kindly provided a FORTRAN deck which was modified and compiled for the Berkeley IBM 709.

In this study, line positions on each film were measured three times to minimize random errors. In several cases the samples had not been mounted properly and a correction for $\Delta\theta_{ecc\perp}$ had to be made. The effect of different extrapolation functions, weighting factors, and ranges of angles used was studied to determine the effect of these variables on the calculated lattice parameters. The lattice constants obtained by different computational methods are listed in Table VI. A low value of V, defined as

$$V = \Sigma w_i V_i^2/(N-K-1)\Sigma w_i, \qquad (6)$$

where w_i = weight, V_i = residual, N = number of reflections, and K = number of parameters, is the criterion for a good fit.

The quality of the x-ray diffraction patterns decreases with increasing temperature, and the high-angle lines are usually poorly resolved at higher temperatures. Because of this it is desirable to use all the reflections rather than just the poorer high-angle lines to calculate the cell constants. Table VI shows that there is only a negligible change in the lattice parameters when all the reflections, instead of only those above 50 deg, are used. The table also indicates that with the samples and camera in this work the choice of extrapolation functions makes very little difference. The Nelson-Riley function gives a slightly lower V and was used in all the calculations. In Fig. 7, $\sin^2\theta_{calc} - \sin^2\theta_{obs}$ is plotted against θ to show the scatter of experimental points about the extrapolation curve for the sample considered in Table VI.

Statistically, the weight used in the least-squares treatment should be $1/\sigma^2$, where σ^2 is the variance. In the above calculations this was approximated by the square of the average deviation of three measurements. Table VI shows that almost the same lattice constants are obtained when each line is assigned unit weight. However, a poorly measured high-angle line can change the calculated a and c by a noticeable amount. The data indicate $\sigma = 0.04$ for the reflection at 83 deg, whereas for most other reflections on the film $\sigma = 0.01 - 0.02$.

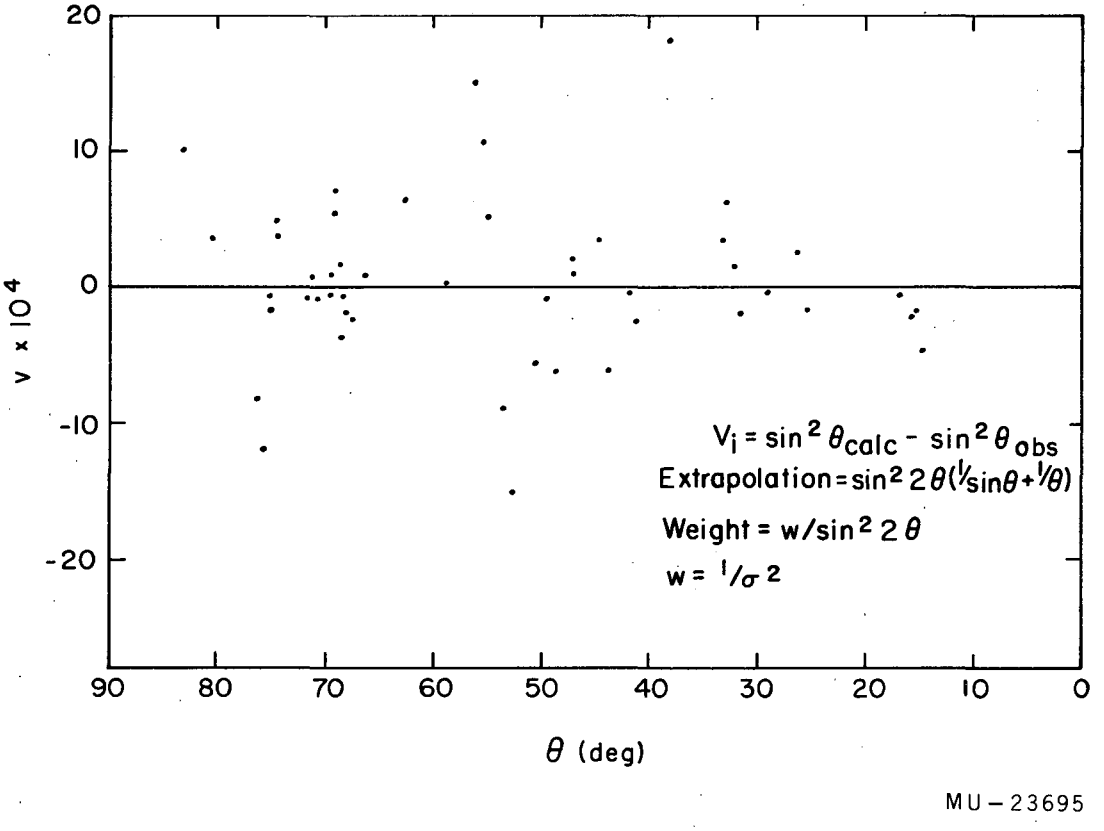

Fig. 7. Plot of V versus θ for dhcp Am metal at 20 °C (Sample 22).

Table VIA. Effect of extrapolation functions on a and c

Parameter	θ (deg)	Extrapolation						
		None	$\sin^2 2\theta$	$\sin^2\theta\sin 2\theta$	$\sin^2 2\theta/2\theta$	$\cos^2\theta\sin\theta$	$\cos^2\theta\sin^2 2\theta$	$D\sin^2 2\theta + E\sin^2 2\theta [(1/\sin\theta + 1/\theta)]$
a A	All	3.46829	3.46815	3.46827	3.46825	3.46824	3.46826	3.46803
95% error		±0.00004	±0.00005	±0.00004	±0.00004	±0.00004	±0.00004	±0.00006
	>50	3.46832	3.4685	3.46839	3.46845	3.46847	3.46837	3.4686
		±0.00005	±0.0001	±0.00007	±0.00009	±0.00009	±0.00006	±0.0002
c A	All	11.2401	11.2395	11.2399	11.2399	11.2399	11.2397	11.2391
95% error		±0.0002	±0.0002	±0.0002	±0.0002	±0.0002	±0.0002	±0.0002
	>50	11.2394	11.2399	11.2396	11.2397	11.2398	11.2395	11.2402
		±0.0003	±0.0003	±0.0003	±0.0003	±0.0003	±0.0003	±0.0005
V x 10^9	All	2.199	2.188	2.228	2.226	2.225	2.170	2.206
	>50	4.218	4.342	4.356	4.351	4.346	4.372	4.529

Table VIB. Effect of weighting factor on a and c

Parameter	θ	Extrapolation: $\sin^2 2\theta[(1/\sin\theta) + (1/\theta)]$ Weight $w_i = 1/\sigma_i^2$ w	$w_i = 1/\sigma_i^2$ $w/\sin^2 2\theta$	$w_i = 1$ except $w_{830}=0.1$ w	$w_i = 1$ except $w_{830}=0.1$ $w/\sin^2 2\theta$	$w_i = 1$ w	$w_i = 1$ $w/\sin^2 2\theta$
a A	All	3.36814	3.46825	3.4684	3.46858	3.4678	3.4680
95% error		0.00006	±0.00004	±0.0001	±0.00007	±0.0004	±0.0002
	$>50^\circ$	3.4684	3.4685	3.4685	3.4686	3.4697	3.4694
		±0.0001	±0.0001	±0.0003	±0.0001	±0.0005	±0.0003
c A	All	11.2396	11.2398	11.2392	11.2382	11.248	11.246
95% error		±0.0003	± 0.0002	± 0.0006	± 0.0003	± 0.002	± 0.001
	$>50^\circ$	11.2393	11.2398	11.239	11.2380	11.238	11.2418
		±0.0005	±0.0003	±0.001	±0.0005	±0.002	± 0.0005
V x 10^9	All	2.617	2.125	8.168	6.542	35.51	22.93
	$>50^\circ$	4.401	4.348	19.54	14.72	67.02	51.58

The line at 83 deg should be given a weight of $w_{83} = (0.015)^2/(0.04)^2 \approx 0.1$ in comparison to the average line. If this is done, the lattice constants agree very well with those calculated by using the observed weights. Therefore, the necessary calculations can be minimized by assigning unit weights to all but the poorest lines without affecting the calculated lattice parameters.

C. Results

The metal prepared by the reduction of americium trifluoride can be indexed as an hexagonal crystal with the c axis double that to be expected for a normal hexagonal close-packed (hcp) structure. The observed and calculated $\sin^2\theta$ obtained from powder patterns taken by using Cu K_a x rays are compared in Table VII. Several different assignments for the high-angle reflections were tried, and those listed in the table gave the best fit. The column headed $V \times 10^5$ is the difference between the calculated and observed $\sin^2\theta$ obtained by using a Nelson-Riley function, and V is plotted against θ in Fig. 7. The lattice parameters calculated for two samples are listed in Table VIII along with the x-ray wave lengths used. The agreement is quite good; however, the absolute error in the cell constants is larger, owing to a 0.01% experimental error in the determination of the effective camera radius from the film. The lattice parameter obtained under similar conditions for a sample of pure gold was a = 4.0779 A at 20°C. The value listed in Wyckoff[38] is a = 4.07864 A at 25°C, or, correcting to 20°C (taking $\alpha = 14.3 \times 10^{-6}/°C$,[39] a = 4.0783 A. The difference of 0.0004 A is within the experimental error of 0.01%, and the lattice constants of americium metal can be given as

$$a = 3.4681 \pm 0.0008 \text{ A}$$
$$c = 11.240 \pm 0.004 \text{ A} \quad (\text{at } 20\,^{\circ}\text{C}).$$

The doubling of the c axis suggests that americium crystallizes in the lanthanum-type structure, which is $P6_3/mmc$ (D_{6h}^4) with metal atoms in 2(a) 000, $00\frac{1}{2}$, and 2(c) 1/3, 2/3, 1/4; 2/3, 1/3, 3/4.

Table VII . Americium metal - dhcp (20°C) - Sample 22)

hk.l	$\sin^2\theta_{calc}$	$\sin^2\theta_{obs}$	V x 10^5	I(calc)	I(obs)
10.0	0.0659	0.0663	-46	11	T
10.1	0.0706	0.0707	-17	62	S
00.4	0.0753	0.0754	-21	50	VS
10.2	0.0847	0.0847	- 6	144	S
10.3	0.1082	0.1082	- 1	35	W
10.4	0.1411	-	-	8	-
10.5	0.1835	0.1836	-17	16	VW
11.0	0.1976	0.1973	26	37	M
10.6	0.2352	0.2352	- 4	33	S
20.0	0.2635	0.2593	-	1	W[a]
20.1	0.2682	-	-	9	-
11.4	0.2729	0.2730	-20	45	S
20.2	0.2823	0.2821	16	24	M
10.7	0.2964	0.2957	62	7	T
00.8	0.3011	0.3006	36	6	M
20.3	0.3058	-	-	7	-
20.4	0.3387	-	-	2	-
10.8	0.3669	-	-	2	-
20.5	0.3811	0.3792	180	5	VW
20.6	0.4328	0.4330	-24	12	W
10.9	0.4469	0.4469	- 4	4	M
21.0	0.4611	-	-	1	-
21.1	0.4658	0.4700	-	7	VW[a]
21.2	0.4799	0.4805	-60	21	W
20.7	0.4940	-	-	3	-
11.8	0.4987	0.4983	35	18	S
21.3	0.5034	-	-	7	-
10.10	0.5363		11	10	
		0.5361			W
21.4	0.5364		24		
20.8	0.5645	0.5651	-60	1	VW
21.5	0.5787	0.5787	- 9	6	T
30.0	0.5928	0.5934	-55	8	VW
21.6	0.6304	0.6321	-17	18	M
10.11	0.6350	-	-	3	-
20.9	0.6445	0.6454	-89	3	T
30.4	0.6681	0.6676	50	16	M
00.12	0.6774	0.6763	108	3	VW
21.7	0.6916	0.6901	151	6	T
20.10	0.7339	0.7338	4	9	VW
10.12	0.7432	-	-	1	-
21.8	0.7621	-	-	2	-
22.0	0.7904	0.7898	65	9	VW
20.11	0.8327	0.8335	-	4	T[a]
21.9	0.8421	0.8420	9	8	VW[a]
31.0 a_1	0.8549	0.8553	-25	0.7	T
31.0 a_2	0.8591	-	-	0.3	-
10.13 a_1	0.8594	0.8598	-38	3	W
31.1 a_1	0.8596		-19	5	
10.13 a_2	0.8637			1	
31.1 a_2	0.8639			3	
22.4 a_1	0.8643	0.8644	- 8	15	S
22.4 a_2	0.8686	0.8684	17	8	T
11.12 a_1	0.8735		56	15	
		0.8730			M
31.2 a_1	0.8737		72	17	
11.12 a_2	0.8779		- 5	8	
		0.8779			T
31.2 a_2	0.8780		11	9	
30.8 a_1	0.8924	0.8925	- 7	17	M
30.8 a_2	0.8968			9	
		0.8971	8	7	W
31.3 a_1	0.8972				
31.3 a_2	0.9016	0.9017	- 9	3	T
21.10 a_1	0.9300		39	25	
		0.9296			M
31.4 a_1	0.9300		49	3	
21.10 a_2	0.9346		-17	13	
		0.9348			VW
31.4 a_2	0.9347		- 7	1	
20.12 a_1	0.9393	0.9405	-117	1	T
20.12 a_2	0.9440	0.9448	- 81	1	T
31.5 a_1	0.9723	0.9720	37	13	VW
31.5 a_2	0.9771	-	-	8	-
10.14 a_1	0.9862	0.9852	104	29	VW
10.14 a_2	0.9911	-	-	18	-

[a] Lines superimpose on americium monoxide lines

This structure has the general line extinction that for reflections with $(h + 2k)/3 = n$ only those with $\ell/4 = m$ are allowed, and this is in agreement with the observed lines. The intensities of the reflections calculated from

$$I = F^2 \rho(1 + \cos^2 2\theta)/\sin^2\theta \cos\theta ,$$

where F = the structure factor and ρ = multiplicity, are listed along with the visual estimates of the intensities of the powder pattern lines in Table VII. With a few notable exceptions the calculated intensities are in reasonable agreement with the observed intensities. The exceptions are the 00.4, 11.0, 11.4, 00.8, 11.8, 11.12 reflections, which are sharper than the average line. The 00.4 reflection appears to be stronger than the 10.2 reflection, but a densitometer tracing shows that this apparent discrepancy is due to the broadening of the 10.2 reflection with respect to the 00.4 reflection. The total intensity of the 10.2 reflection is greater than that of the 00.4 reflection. However, the background on the films is high, and the signal-to-noise ratio of the densitometer tracing is not large enough to permit a quantitative comparison of the line widths. As discussed in the section on metal preparation, similar phenomena have been observed in cobalt and have been attributed to stacking faults in the sequence of hexagonal layers which make up a close-packed structure.[18] Wilson has shown that the lines with $(h-k)/3 = n$ will be sharp and the remaining lines broadened by an amount which is dependent on the average number of stacking faults per N hexagonal layers.[19] More recent work on cobalt indicates that there are several types of faults that can occur and that the hcp phase obtained by cooling through the fcc phase contains 25 to 30 % of the parent fcc phase.[40] The diffraction patterns of americium metal do not show lines that would correspond to the 200 and 331 fcc reflections (the stronger lines which do not superimpose on the dhcp reflections), indicating that very little of the fcc phase remains in the dhcp phase at room temperature. A more detailed discussion of stacking

Table VIII. Comparison of a and c (in A) for Samples 19 and 22

	Sample 19		Sample 22		
Film	1	2	1	2	Cu wave lengths
a	3.4673	3.4687	3.4680	3.46825	$CuK\alpha_1$ = 1.54051
95% error	±0.0001	±0.0001	±0.0002	±0.00004	$CuK\alpha_2$ = 1.54433
c	11.2399	11.2402	11.246	11.2398	$CuK\bar{\alpha}$ = 1.54178
95% error	±0.0002	±0.0006	±0.001	±0.0002	
V x 10^9	5.342	10.10	22.93	2.125	
					Absolute Lattice Constants
a ave.	3.4680 ±0.0007		3.46813 ±0.0002		3.4681 ±0.0008
c ave.	11.2401 ±0.0006		11.2402 ± 0.0010		11.240 ±0.004

faults is beyond the scope of this work. Also, the quality of the films obtained in this study is not sufficient to make a quantitative estimate of the number and nature of the stacking faults, but the apparent differences in the observed and calculated intensities are compatible with the presence of stacking faults in the metal.

The proposed structure yields a density of 13.671 ±.005 g/cm^3. Each americium has six nearest neighbors at 3.468 A and six at 3.450 A, which gives a metallic radius for coordination number 12 of 1.730 A.

The metal prepared by reduction of americium oxide with lanthanum gave a diffraction pattern which was indexed as fcc with a few stacking faults as evidenced by the appearance of six hcp lines. A typical pattern of a sample collected on tantalum is shown in Table IX, and the calculated lattice constant is 4.898 ±.001 A. A similar coating of americium condensed on quartz gave a lattice constant of 4.890 ±.002 A. The average (a = 4.895 ±.005A) gives a calculated density of 13.65 ±.05 g/cm^3 and a metallic radius of 1.73 A (CN 12). By collecting the americium on a tantalum wire or a quartz fiber, a high-temperature or normally unstable fcc phase is apparently quenched to room temperature.

The americium metal coating on a tantalum wire was studied in a commercial Von der Heyde 57.3-mm-radius high-temperature camera. No structure change was observed up to 360 °C. The results are listed in Table X and plotted in Fig. 8. The films were quite dark because of the x rays resulting from the decay of the americium, and the lattice parameters are not very accurate. An approximate coefficient of thermal expansion for the fcc phase between 22 °C and 360 °C is calculated to be $(9 \pm 3)10^{-6}$ C .

Table IX. Americium metal on tantalum, 22°C

Observed		fcc			dhcp			bcc(Ta)	
I	$\sin^2\theta$	Σh_i^2	I	$Vx10^4$	hk.l	I	$Vx10^4$	Σh_i^2	$Vx10^4$
VW	0.0724				10.1	62	-3		
VS	0.0759	3	50	-4	00.4	50	4		
W	0.0856				10.2	145	6		
S	0.1007	3	26	-3					
M-	0.1100							2	-3
VS	0.1997	8	19	2	11.0	38	-2		
W	0.2187							4	1
W	0.2355				10.6	33	4		
VS	0.2743	11	22	-0.3	11.4	45	-1		
VS	0.2824				20.2	24	15		
S	0.2997	12	6	-7	00.8	7	10		
S	0.3277							6	-0.1
T	0.3964	16	3	17					
W	0.4358							8	7
M	0.4721	19	10	2					
VW	0.4810				21.2	21	-3		
VS	0.4947	20	9	-9	11.8	18	-5		
M	0.5453							10	-1
S	0.5958	24	8	2	30.0	8	-27		
VW	0.6313				21.6	18	-20		

Table IX (cont.)

I	$\sin^2\theta$	Σh_i^2	I	$Vx10^4$	hk.l	I	$Vx10^4$	Σh_i^2	$Vx10^4$
W	0.6540							12	-1
VS	0.6697	27	3	-3	00.12	3.1	26		
					30.4	16.	-24		
Sa_1	0.7610							14	3
Ma_2	0.7654							14	-4
Wa_1	0.7922	32	5	-0.6	22.0	9.	-43		
VWa_2	0.7934	32	3	-21	22.0	5	-21		
VSa_1	0.8659	35	23	1	31.2	26	-56		
					11.12	23	10		
Ma_2	0.8705	35	12	-2	31.2	13	-54		
					11.12	12	7		
Sa_1	0.8907	36	16	-0.4	30.8	25	-25		
Wa_2	0.8963	36	8	-12	30.8	13	-37		

fcc a = 4.898 ± 0.001

dhcp a = 3.474 ± 0.002

c = 11.30 ± 0.01

bcc a = 3.304 ± 0.001

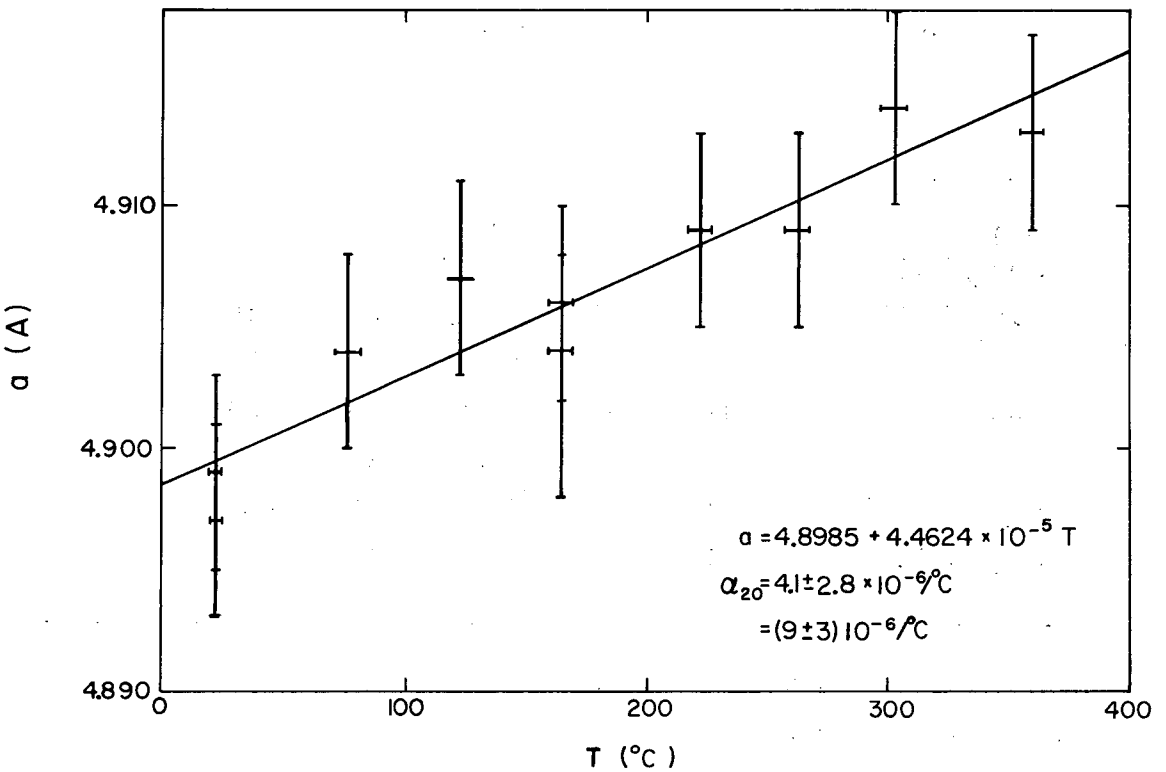

Fig. 8. Plot of a versus T for fcc Am on Ta.

Table X. Variation in a with temperature for fcc Am on Ta

T (^{o}C)	a (A)
22 ± 1	4.897 ± 0.004
22 ± 1	4.899 ± 0.004
76 ± 10	4.904 ± 0.004
123 ± 10	4.907 ± 0.004
165 ± 10	4.906 ± 0.004
165 ± 10	4.904 ± 0.004
222 ± 10	4.909 ± 0.004
263 ± 10	4.909 ± 0.004
303 ± 10	4.914 ± 0.004
360 ± 10	4.913 ± 0.004

A far more extensive study was made at high temperatures on the pure, bulk-phase metal produced by the reduction of americium trifluoride by using the techniques described in the preceding two sections. The metal has been studied from -120 ^{o}C to 605 ^{o}C and the results obtained from two samples are listed in Table XI. The data were fitted to a polynomial of second order in temperature by the method of least squares. The data are not sufficiently accurate to warrant higher terms. The average values from the two sets of equations are plotted in Figs. 9 and 10 for the a and c parameters respectively. The calculated coefficients of thermal expansion at 20 ^{o}C are

$$\left.\begin{aligned} \alpha_a &= 7.5 \pm .2\times10^{-6}/\,^{o}\text{C} \\ \alpha_c &= 6.2 \pm .4\times10^{-6}/\,^{o}\text{C} \end{aligned}\right\} \quad \text{(at } 20\,^{o}\text{C)} \ .$$

Up to 605 ^{o}C there is no definite indication of any change in structure, only the expected general decrease in the intensities of the diffraction-pattern lines. The intensities of both samples at 20 ^{o}C and approx 600 ^{o}C are listed in Table XII.

Table XIA. Thermal expansion of dhcp americium metal--Sample 19

T (^{o}C)	a (A)	c (A)	V x 10^{8}
20	3.4673 ± 0.0001	11.240 ± 0.001	0.534
20	3.4686 ± 0.0001	11.240 ± 0.001	1.01
133	3.4725 ± 0.0003	11.254 ± 0.001	2.95
256	3.4738 ± 0.0004	11.264 ± 0.001	2.84
361	3.4772 ± 0.0003	11.263 ± 0.001	2.46
446	3.4808 ± 0.0003	11.278 ± 0.001	3.37
471	3.4793 ± 0.0005	11.288 ± 0.001	4.81
500	3.4824 ± 0.0005	11.292 ± 0.002	4.27
528	3.4819 ± 0.0004	11.289 ± 0.001	3.30
560	3.4850 ± 0.0006	11.302 ± 0.002	6.37
604	3.4823 ± 0.0004	11.293 ± 0.002	3.31
605	3.4863 ± 0.0008	11.307 ± 0.003	7.69

Extrapolation: $D \sin^2 2\theta + E \sin^2 2\theta ((1/\sin\theta) + (1/\theta))$

Weight: $1/\sin^2 2\theta$

$a_T = 3.4671 + 2.62 \times 10^{-5} T + 0.56 \times 10^{-8} T^2$

$c_T = 11.238 + 6.59 \times 10^{-5} T + 6.3 \times 10^{-8} T^2$

Table XIB. Thermal expansion of dhcp americium metal--Sample 22

T (^{o}C)	a (A^{o})	c (A)	V x 10^{8}
-121[a]	3.4654 ± 0.0001	11.228 ± 0.001	0.984
-97[a]	3.4640 ± 0.0001	11.227 ± 0.001	0.598
-50	3.4679 ± 0.0001	11.236 ± 0.001	1.19
20	3.4680 ± 0.0002	11.246 ± 0.001	2.29
20	3.4685 ± 0.0001	11.238 ± 0.001	1.42
107	3.4708 ± 0.0001	11.243 ± 0.001	1.19
185	3.4736 ± 0.0001	11.256 ± 0.001	1.33
284	3.4761 ± 0.0002	11.259 ± 0.001	2.96
287	3.4754 ± 0.0002	11.266 ± 0.001	2.94
407	3.4773 ± 0.0003	11.274 ± 0.001	7.35
510	3.4806 ± 0.0004	11.295 ± 0.002	5.70
512	3.4809 ± 0.0003	11.294 ± 0.002	4.06
517	3.4805 ± 0.0003	11.293 ± 0.001	3.28
584	3.4845 ± 0.0003	11.303 ± 0.001	3.86
588	3.4843 ± 0.0004	11.308 ± 0.001	4.26

Extrapolation: $E \sin^2 2\theta \left((1/\sin\theta) + (1/\theta) \right)$

Weight: $1/\sin^2 2\theta$

[a]Extrapolation: $D \sin^2 2\theta + E \sin^2 2\theta \left((1/\sin\theta) + (1/\theta) \right)$

$a_T = 3.4673 + 2.57 \times 10^{-5} T + 0.52 \times 10^{-8} T^2$

$c_T = 11.236 + 7.31 \times 10^{-5} T + 7.3 \times 10^{-8} T^2$

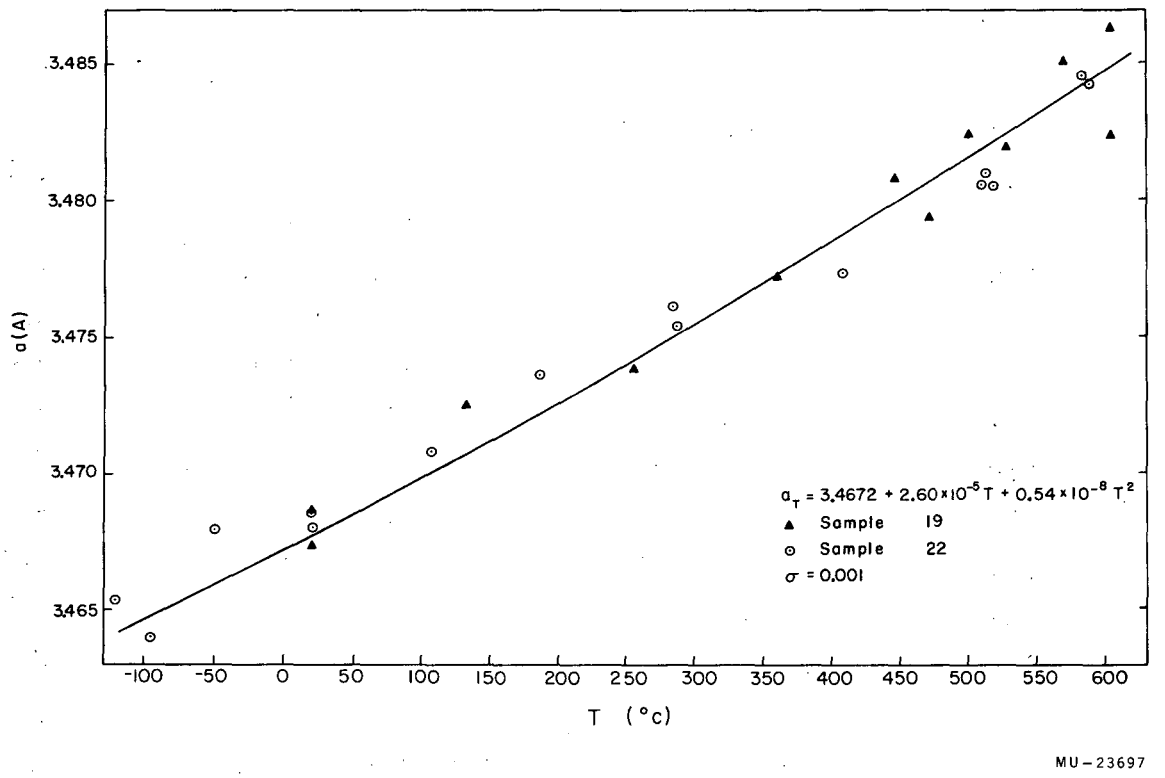

Fig. 9. Thermal expansion of americium metal along the a axis.

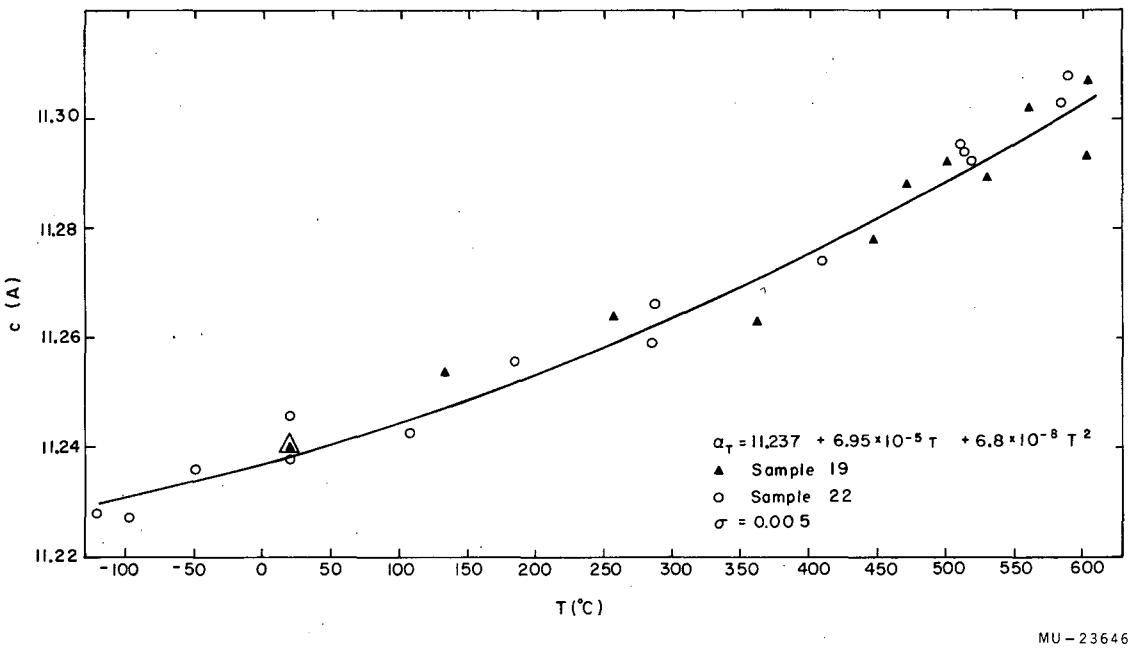

Fig. 10. Thermal expansion of americium metal along the c axis.

Table XII. Comparison of the line intensities at 20 °C and 600 °C

hk.l	Sample 22		Sample 19		hk.l	Sample 22		Sample 19	
	20°	584°	20°	605°		20°	584°	20°	605°
10.0	T	VW	VW	T	21.6	M	M	S	M
10.1	S	S	S	S	20.9	T	-	VW	-
00.4	VS	VS	VS	S	30.4	M	T	W	-
10.2	S	S	M	W	00.12	VW	-	W	-
10.3	W	W	W	VW	21.7	T	T	-	T
10.5	VW	T	W	-	20.10	VW	-	-	-
11.0	M	W	VW	T	22.0	VW	-	-	-
10.6	S	M	S	W	21.9	VWa_1	-	-	-
11.4	S	S	S	W	31.0	Ta_1	-	-	-
20.2	M	M	M	W	31.1	Wa_1	Wa_1	VWa_1	-
10.7	T	VW	-	-	22.4	Ma_1+a_2	Ta_1	Wa_1	-
00.8	M	W	M	W	11.12	Sa_1	Wa_1	Sa_1	Wa_1
20.5	VW	VW	T	-		Wa_2	VWa_2	Wa_2	VWa_2
20.6	W	VW	VW	-	30.8	Ma_1	VWa_1	Wa_1	VWa_1
10.9	M	VW	S	M	31.3	Wa_1+a_2	Ta_1	VWa_1	-
21.2	W	W	T	W	31.4	Ma_1+a_2	-	-	Ta_1
11.8	S	M	S	W	20.12	Ta_1a_2	-	-	-
21.4	W	T	W	-	31.5	VWa_1	-	-	-
20.18	VW	VW	W	W	10.13	VWa_1	-	-	-
21.5	T	T	T	T					
30.0	VW	T	-	T					

Diffraction patterns were obtained at 700 °C and 850 °C by wrapping the film around the oven, as described earlier. The patterns were poor, and there was some oxidation of the sample and vaporization onto the capillary walls. The x-ray data obtained at 850 °C are presented in Table XIII. The film was calibrated against the tantalum lines, but the fluctuations in the measured angles of the lines was still quite large. Most of the lines can be indexed as bcc tantalum or fcc americium monoxide. Seven of the remaining twelve lines could be interpreted as fcc with a = 4.91 A, approximately the value expected for a fcc americium metal phase on the basis of the coefficient of thermal expansion for the fcc phase presented above. The other five lines may be oxide lines, but such an assignment is even more tenuous than the assignment of the fcc phase. An x-ray diffraction pattern obtained in the regular camera after the high-temperature run showed much stronger americium monoxide lines; the lines indexed as fcc with a = 4.91 A either had disappeared or were much weaker, and the other five lines showed little change. The pattern obtained at 700 °C was very similar to that obtained at 850 °C. These data imply that a transition from dhcp to fcc occurs between 600 ° and 700 °C, but the evidence is at best marginal. The fact that vaporized metal that had collected on a tantalum wire or quartz fiber and cooled to room temperature was predominantly fcc is further evidence for the existence of a fcc phase at high temperatures. However, until the problem of obtaining high-temperature x-ray diffraction patterns from this reactive, volatile metal is solved, no more definite statement about the transition from dhcp to fcc in americium metal can be made.

Table XIII. Sample 23--38-mm-diameter camera--850 °C

I	$\sin^2\theta$	bcc Ta		fcc AmO		fcc Am	
		Σh^2	$\sin^2\theta$	Σh^2	$\sin^2\theta$	Σh^2	$\sin^2\theta$
T	0.055						
W	0.068			3	0.068		
VW	0.076					3	0.074
W	0.091			4	0.091		
VW	0.108	2	0.108				
T	0.129						
VW	0.143						
T	0.163						
VW	0.182			8	0.181		
T	0.220	4	0.215				
T	0.294					12	0.296
T	0.323	6	0.323				
T	0.353			16	0.363		
VW	0.429	8	0.430	19	0.431		
VW	0.460			20	0.454	19	0.469
W	0.486					20	0.493
W	0.518						
VW	0.541	10	0.538				
VW	0.676					27	0.666
W	0.726			32	0.726		
W	0.753	14	0.753				
T	0.781					32	0.789
M	0.805			35	0.793		
M	0.828			36	0.817		
VW	0.856	16	0.860				
VW	0.874					35	0.863
VW	0.887					36	0.888
VW	0.916			40	0.907		

bcc Ta: a = 3.32 A
fcc AmO: a = 5.12 A
fcc Am: a = 4.91 A

V. MAGNETIC SUSCEPTIBILITY MEASUREMENTS

A. Experimental

Cunningham[41] has described an apparatus used to measure the magnetic susceptibility of submicrogram quantities of the +3 ions of berkelium and californium. This apparatus was modified to measure the susceptibility of americium metal. The susceptibility is measured by a modified Faraday method in which the sample, suspended on a long quartz fiber, is exposed to an inhomogeneous magnetic field. The principle of this method is sketched in Fig. 11. If the fiber is of uniform cross section and infinitely flexible and if the sample is placed midway between the pole faces of the magnet in the y direction $(\partial H/\partial y) = 0$, then the equilibrium position of the sample is given by

$$d = \frac{K \Sigma m_i \chi_i}{\Sigma m_i + C + D \Sigma m_i \chi_i} ,$$

where

$$K = \frac{\ell H_x}{g} \left(\frac{\partial H}{\partial x}\right) ,$$

$$C = m_f/2 ,$$

$$D = \frac{H_z}{g} \left(\frac{\partial H}{\partial z}\right)$$

χ_i = gram susceptibility of ith component of the sample,

m_i = mass of the ith component,

ℓ = length of the suspension fiber,

m_f = mass of the fiber,

H_x, H_z = magnetic field components in the x and z directions, respectively,

$\left(\frac{\partial H}{\partial x}\right)$, $\left(\frac{\partial H}{\partial z}\right)$ = field gradients in the x and y directions respectively.

If the sample is very small, then it can be suspended so that $\left(\frac{\partial H}{\partial z}\right) \approx 0$. This can also be accomplished for a larger sample by making the

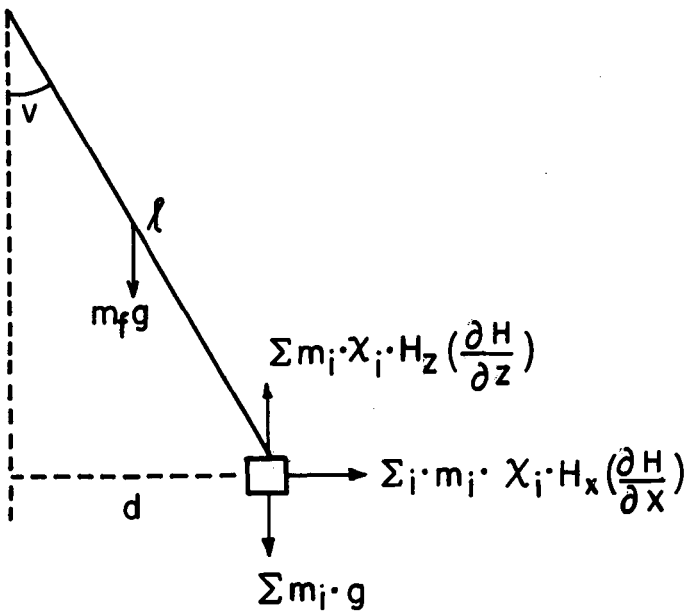

Fig. 11. Principle of magnetic susceptability apparatus.

magnet pole faces longer in the z direction. The latter was done in the present work, and the equation for the deflection of the sample in a magnetic field reduces to

$$d = \frac{K \Sigma m_i \chi_i}{\Sigma m_i + C} \quad . \tag{7}$$

There are two apparatus constants to be determined. A material of known susceptibility is used, and two independent experiments performed. In each one the deflection, d_i^o, of an empty tube of mass m_i^o is measured (this includes the weight of the hook from which the sample tube is suspended, which is also in the magnetic field). Then, the deflection d_i of the tube containing m_i grams of a substance of known gram susceptibility, χ_i, is determined. From these measurements two equations can be written,

$$d_i^o = K m_i^o \chi_i / (m_i^o + C) \quad ,$$

$$d_i = K(m_i^o \chi_i^o + m_i \chi_i)/(m_i^o + m_i + C),$$

where χ_i^o is the unknown susceptibility of the blank tube and hook. The χ_i^o can be eliminated to give an equation of the form

$$d_i = \frac{(m_i^o + C)}{(m_i^o + m_i + C)} d_i^o + \frac{m_i K \chi_i}{(m_i^o + m_i + C)} \quad . \tag{8}$$

If two independent experiments are performed, then the equations can be solved for K and C:

$$K = \frac{[(m_2^o - m^o)(d_2^o - d_2^o)(d_1^o - d_1) + m_1 d_1 (d_2^o - d_2) - m_2 d_2 (d_1^o - d_1)]}{[m_1 \chi_1 (d_2^o - d_2) - m_2 \chi_2 (d_1^o - d_1)]} \quad ,$$

$$C = \frac{m_1 \chi_1 [m_2 d_2 - m_2^o (d_2^o - d_2)] - m_2 \chi_2 [m_1 d_1 - m_1^o (d_1^o - d_1)]}{[m_1 \chi_1 (d_2^o - d_2) - m_2 \chi_2 (d_1^o - d_1)]} \quad ,$$

where the subscripts refer to the different experiments. The standardization can be simplified by using the same tube and either two weights

of the same standard material or measurements on one sample at two temperatures. In practice, however, C usually is small compared with $(m_i + m_i^o)$, and no appreciable error is introduced by using a fiber mass which has been calculated from the density of quartz and the volume of the fiber as computed from its length and diameter. In this way the constant K can be determined at different field strengths in one experiment, using Eq (8). Nickelous ammonium sulfate, $Ni(NH_4)_2(SO_4)_2 \cdot 6H_2O$, has been suggested as a reliable standard for susceptibility measurements.[42] Nickelous ammonium sulfate crystals from Baker and Adamson lot #7 were vapor-equilibrated with a saturated solution of $Ni(NH_4)_2(SO_4)_2 \cdot 6H_2O$, and the measurements made at three temperatures. The apparatus constants were determined by taking[43]

$$\chi_g(Ni(NH_4)_2(SO_4)_2 \cdot 6H_2O) = \left(\frac{3174}{T+2.5} - 0.30\right) 10^{-6} \text{ erg/gauss}^2 \quad .$$

The constants were also determined by using freshly ignited neodymium sesquioxide ($\chi_g = 30.3 \times 10^{-6}$ erg/gauss^2 at 292°K).[44]

The apparatus is sketched in Fig. 12. The fiber is supported on a removable ring mounted on a micrometer which allows the deflections to be measured by a null method in which the sample is always restored to the same position in the magnetic field. In this way possible errors resulting from variations in $H(\partial H/\partial x)$ with sample position are minimized. The suspension fiber can also be rotated to bring an asymmetric sample to a position of zero rotational torque in the magnetic field. The deflection of the sample is observed through the telescope system. It is restored to its initial position with reference to a hair line in the filar micrometer by adjusting the micrometer attached to the fiber suspension. The micrometer can be read to an estimated ±0.02 mil. The field was produced by an electromagnet with pole faces shaped to give an inhomogeneous magnetic field, and the susceptibility of the sample was determined at six different current settings with $H_x(\partial H/\partial x)$ varying from 9.5×10^5 to 43.4×10^5 gauss^2/cm. This enabled a correction to be made for any ferromagnetic impurities present

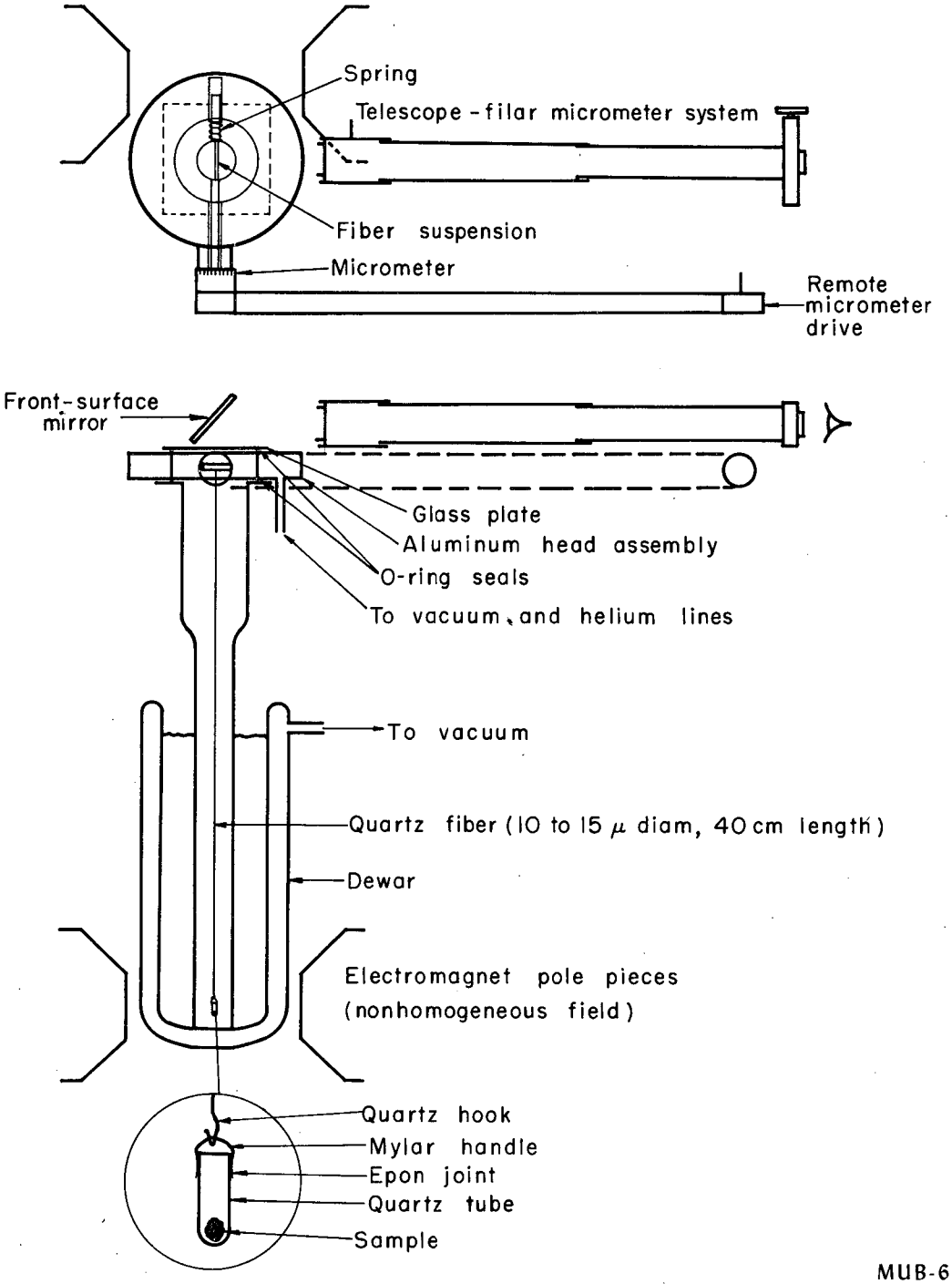

Fig. 12. Magnetic susceptibility apparatus.

in the sample and made it possible to detect any magnetic transitions in the sample. All measurements were made under 1/3 atm of helium. The following constant-temperature baths were used:

ice-H_2O	0°C
Freon 22 (momochlorodifluoromethane)	-40.8°C
alcohol—dry ice	-72 °C
methylcyclohexane slush	-126 °C
liquid nitrogen	-195.8°C

For these measurements the sample was placed in a quartz tube with a polyethylene or Mylar handle held on with epon. In order to make high-temperature measurements, the sample was suspended in a quartz tube which was surrounded by an oven consisting of a copper block heated by a platinum winding. The sample was sealed in vacuum in a capillary having a quartz eye on one end with which to hook the sample on the fiber. This method has the disadvantage that the diamagnetic correction for the sample tube could not be determined experimentally, and it had to be calculated from its weight and the literature value for the susceptibility of quartz.

The major problem in the measurement of the magnetic susceptibility of milligram samples of metal is the contamination of the sample with trace amounts of ferromagnetic impurities. Care must be taken to use only gold-tipped forceps and a tungsten needle to clean the sample. Even with these precautions, several of the samples apparently contained ferromagnetic impurities since the susceptibility was found to be slightly field-dependent. In the presence of these impurities the susceptibility of the metal was determined by extrapolating the apparent susceptibility against the reciprocal of the current to $1/i = 0$. This is equivalent to extrapolating to infinite magnetic field, where the ferromagnetic impurity is saturated and does not contribute to the measured susceptibility.

Several of the samples contained embedded tantalum wire as a result of the method of preparation. The tantalum and the americium were run together, and then the americium was dissolved in acid and assayed. The tantalum remaining was reweighed and run in the sample tube to determine the diamagnetic correction.

B. Results

The magnetic susceptibilities of six samples of americium metal have been investigated, and the results are listed in Table XIV. The purity of the samples and the experimental conditions varied greatly. The sample numbers refer to the preparations listed in Table III for which the results of analysis are listed in Table IV. The last column of Table XIV indicates the field dependence shown by some of the samples. The relation between the magnetic field and the current is estimated to be $dH/di \approx 5000 \pm 2000$ gauss/amp. As pointed out in the legend, Samples 9, 17, and 13 were run in an earlier form of the apparatus. The pole faces were not longer in the z direction than in the x direction (Fig. 11), and the apparatus constant was deflection-dependent, as shown by standardizations made by using different quantities of Mohr's salt. These samples were also sealed in quartz capillaries. Samples 28, 27, and 25 are of higher purity, and the apparatus had been modified to reduce the shape factor or apparent dependence of the constant on the deflection. The error in the apparatus constants varied from 3.3% to 2.7%, depending on the current setting. The absolute error in the susceptibility of the standard materials used in the standardization was assumed to be 2%, and this assumption accounts for most of the error in the apparatus constants. The best value for the magnetic susceptibility of americium metal at 20°C is

$$\chi_{20^\circ C} = (881 \pm 46) \times 10^{-6} \text{ erg/gauss}^2\text{/mole.}$$

Measurements made below and above room temperature are reported in Table XV. There is a large scatter in the values below room temperature. The scatter occurs because the change in susceptibility in the range from -196°C to 20°C is very small and well

Table XIV. Magnetic susceptibility of americium metal

Sample	$\chi_{20^oC} \times 10^6$ ergs/gauss^2/mol	Mol %Am	Weight (mg.)	$d\chi/d(1/i)$
28[a,b]	881 ± 32	99.8	2.529	-
27[b]	876 ± 55	98.5	0.336	-
25[a,b]	885 ± 50	96.9	3.423	175
9[c,d]	900 ± 100	94.4	0.631	1780
17[c,d]	928 ± 100	89.6	1.028	103
13[c,d]	738 ± 100	88.7	1.295	519

[a]Samples 28 and 25 were measured with tantalum and corrected with a blank run.

[b]Samples 25, 27, and 28 were run with a fiber calibrated against $Ni(NH_4)_2(SO_4)_2 \cdot 6H_2O$ and Nd_2O_3.

[c]Samples 9, 17, and 13 were sealed in quartz capillaries, and the gram susceptibility of quartz was assumed to be -0.493×10^{-6} cgs units.

[d]Samples 9, 17, and 13 were run with a fiber calibrated against $Fe(NH_4)_2(SO_4)_2 \cdot 6H_2O$, and used the small pole faces, which resulted in an apparent shape factor.

Table XV. Temperature dependence of the susceptibility of americium metal

	$100(\chi_T - \chi_{20})/\chi_{20}$				
Sample	0°C	-40.8°C	-72°C	-126°C	-196°C
28	0.5± 0.8	0.3± 1.1	0.9± 1.1	1.2± 1.0	1.2± 0.9
27	-	-	-	-	-2.0± 1.1
25	- 0.3± 5.0	0.3± 5.0	-1.0± 5.0	-2.4± 5.0	-1.0± 5.0
9	-4.5± 10	-	-	-	2.2± 10 -5.6± 10
17	0.8± 5.0	-	-0.1± 5.0	-	0.5± 5.0
13	1.1± 5.0	-	-	-	3.3± 5.0

Sample 9–Susceptibility of americium metal above room temperature

T(°C)	$\chi_T 10^6$	T(°C)	$\chi_T 10^6$
20	900± 100	100	890± 100
50	880± 100	125	960X100
75	840± 100	150	910± 100
100	850± 100	175	910± 100
125	850± 100	200	940± 100
150	870± 100	250	900± 100
200	880± 100	300	890± 100
250	880± 100	350	900± 100
300	870± 100	400	880± 100
350	920± 100	450	880± 100
17	890± 100	550	940± 100

below the experimental error for the samples that required an extrapolation to remove the field dependence. The best sample (28) does show a consistent increase in the susceptibility with decreasing temperature. However, all that can be said on the basis of all the data is that there is less than 2% change in the susceptibility of americium metal between -196 and 20°C. The high-temperature measurements made on Sample 9 also show no change above the experimental error, and it is reasonable to set a limit to the temperature dependence between room temperature and 550°C to $\lesssim 5\%$. In the temperature range studied, there is no evidence for any magnetic transitions.

C. Magnetic Susceptibility of Am(III)

The magnetic susceptibility of the rare earth metals is very similar to that of the +3 ions at room temperature. Also, the susceptibility calculated for a configuration of equivalent 4f electrons in the Russell-Saunders limit agrees quite well with these experimental results. For these reasons it is of interest to compare the susceptibility of americium metal with that of Am(III). Two determinations of the susceptibility of Am^{+3} have been reported in the literature. Howland and Calvin measured the susceptibility of the +3 ion in solution and gave $\chi = 720 \times 10^{-6}$ erg/gauss^2/mole at room temperature.[45] Crane et al. measured the susceptibility of americium trifluoride at three temperatures. Their results (corrected for diamagnetism of the fluoride and an estimated diamagnetism of -0.5 for Am^{+3}) are

$$\chi_{295^\circ K} = 1040 \pm 300 \times 10^{-6} \text{ erg/gauss}^2\text{/mole},$$

$$\chi_{199^\circ K} = 1290 \pm 300$$

$$\chi_{77^\circ K} = 1740 \pm 300$$

The limits of error in these measurements were rather large because of a combination of the use of small samples and the small molar susceptibility of Am(III). In the work reported here several additional attempts were made to determine the susceptibility of Am(III).

In the measurement of the susceptibility of the +3 ions of berkelium and californium, Cunningham[41] suggested the use of a single bead of a cation-exchange resin as a suitable matrix. The susceptibility of the berkelium and californium was determined relative to a standard, gadolinium. The diamagnetism of the bead was determined, and then the appropriate ion was absorbed and the deflection, measured. In the study reported herein, single beads of Dowex-50 exchange resin approx 1 mm in diameter were used. Attempts to seal the bead to a quartz rod with epon were unsuccessful. When the bead was stripped with 6 M HCl, it contracted and separated from the epon. Also, the beads cracked after one or two experiments. Finally, small Mylar buckets were made, and the bucket plus bead washooked onto the fiber.

The experiment is complicated by a difference in the water content of the bead when it is in the hydrogen form and when it is saturated with a +3 ion. This difference was determined by weighing the bead with and without the ion absorbed (the weighing conditions were reproduced as closely as possible). The amount of americium was determined by alpha assay, and the observed difference between two beads was

	Bead 1	Bead 2
Assay	89.1 micrograms	92.5 micrograms
Weight change	81.8 micrograms	81.1 micrograms

This amounts to the loss of 1 to 1.5 moles of water for each mole of americium absorbed. A bead was saturated with Sm^{+3} and the susceptibility determined. The amount of Sm^{+3} was measured by the change in weight of the bead and was corrected for the loss of 1.5 moles of water. A similar measurement was made on a new bead with americium. The ratio of the apparent gram susceptibility of Am(III) and Sm(III) was

$$\chi_{Am^{+3}}/\chi_{Sm^{+3}} = 0.404 \pm 0.060 \text{ at } 20^{\circ}C.$$

Using the value of the susceptibility of Sm^{+3} determined by Spedding,[47] one has

$$\chi_{Sm^{+3}} = 1035 \times 10^{-6} \text{ cgs units at } 300^{\circ}K.$$

The molar susceptibility of Am(III) is

$$\chi_{Am^{+3}} = 670 \pm 100 \times 10^{-6} \text{ erg/gauss}^2\text{/mole.}$$

The probable error is large, owing to uncertainty in the amount of sample and water present. Also, there appears to be some trend in the ratio of the susceptibilities with increasing magnet current. Measurements made at liquid nitrogen temperature showed a slight increase in the susceptibility of Am^{+3} with decreasing temperature:

$$\chi_{77}/\chi_{298} = 11 \pm 1\%$$

An attempt was made to grow a crystal of americium ethylsulfate and to determine its susceptibility. Several yellow crystals were grown. However, the apparent susceptibility changed with time, indicating that decomposition of the crystal resulting from the decay of the americium was taking place. When the crystals were dissolved, alpha assay indicated an apparent molecular weight of 468 instead of 778.

It is difficult to find a suitable matrix that will not be destroyed by the radioactivity and yet will keep the ions sufficiently far apart to eliminate magnetic interactions. The low susceptibility of Am^{+3} makes it difficult to accurately determine the susceptibility of the ion if it is diluted by a diamagnetic matrix such as lanthanum trichloride.

The susceptibility of a sample of americium trifluoride was determined, and the results are listed in Table XVI. These results differ by a factor of two from the value reported by Crane et al.[46], but the percent change in the susceptibility between 20°C and -196°C is within the experimental error. The purity of the sample used in this work is probably quite high, and the apparatus has been checked by using two independent standard substances. The apparatus and standardizations were the same ones used for the susceptibility measurements

Table XVI. Magnetic susceptibility of americium trifluoride.

T (°C)	χ_{AmF_3} ($\times 10^{-6}$ erg/gauss^2/Mol)	$\chi_{Am^{+3}}$[a] ($\times 10^{-6}$)
20	487±15	566
0	485±15	564
-72	488±15	567
-196	769±25	848

[a] corrected for diamagnetism of fluoride, -11×10^{-6}, and americium, -46 ± 10^{-6} (Ref. 48).

on americium metal Samples 25, 27, and 28. Fluoride from the same precipitation had been used in successful preparations of pure metal; the success indicated that there were no gross impurities present. The sample was dissolved in nitric acid and alpha-assayed after susceptibility measurements had been made, and there was no difference within experimental error in the amount of americium trifluoride as determined by weight and by alpha assay (2.165±.001 mg by weight and 2.15±.02 mg by assay). It is possible that small amounts of paramagnetic impurities may account for the high value obtained in the earlier work. However, it is evident that a careful determination of the susceptibility of Am^{+3} in a dilute matrix not containing water or organic derivatives is needed.

D. Calculation of the Magnetic Susceptibility of Am(III) and Pu(III)

As mentioned above, in the rare earth region the susceptibility calculated for a configuration of equivalent 4f electrons in the Russell-Saunders approximation agrees very well with the experimental results. In the actinide elements, however, there are marked deviations from pure Russell-Saunders coupling, and it is necessary to extend the formula derived by Van Vleck for the magnetic susceptibility of the rare

earth ions to the intermediate field in order to obtain reasonable agreement with the experimental results.

Van Vleck has shown that for a configuration in which the multiplet intervals are comparable to kT the susceptibility is given by[49]

$$\chi = \frac{N\mu_B^2 \sum_J \{[g_J^2 J(J+1)/3kT] + \alpha_J\}(2J+1)e^{-W_J^0/kT}}{\sum_J (2J+1)e^{-W_J^0/kT}} \qquad (9)$$

where

$$g_J = 1 + \frac{S(S+1) + J(J+1) - L(L+1)}{2J(J+1)}$$

$$\alpha_J = \frac{1}{6(2J+1)} \left[\frac{F(J+1)}{h\nu(J+1;J)} - \frac{F(J)}{h\nu(J;J-1)} \right] ,$$

$$F(J) = \frac{1}{J} \left[(S+L+1)^2 - J^2 \right] \left[J^2 - (S-L)^2 \right] .$$

The functions g_J and α_J are derived from the matrix elements $\langle JM | L_z + 2S_z | J'M' \rangle$, and the only nonzero matrix elements are given by the Wigner-Eckart theorem:

$$\langle JM | L_z + 2S_z | JM \rangle = \langle J || \underset{\sim}{L} + 2\underset{\sim}{S} || J \rangle M$$

$$\langle J+1, M | L_z + 2S_z | JM \rangle = \langle J+1 || \underset{\sim}{L} + 2\underset{\sim}{S} || J \rangle \sqrt{(J+1)^2 - M^2}$$

$$\langle J-1, M | L_z + 2S_z | JM \rangle = \langle J-1 || \underset{\sim}{L} + 2\underset{\sim}{S} || J \rangle \sqrt{J^2 - M^2} .$$

The spin-orbit coupling which splits the LS terms into J levels also couples together states of the same J but different S and L, causing departures from Russell-Saunders coupling.[50] The operator (L_z+2S_z) in the matrix elements above will not couple states of different L and S, so the reduced matrix element for the perturbed level can be expressed as a linear combination of the reduced matrix elements of the

different LS terms. The functions g_J and a_J can then be redefined in the intermediate field for an eigenfunction of the form

$$|\psi_J\rangle = \sum_{L,S} a_{L,S,J} |\psi_J(L,S)\rangle \quad ,$$

as

$$g_J = \sum_{L,S} a_{L,S,J}{}^2 g_J(L,S), \tag{10}$$

$$a_J = \sum_{L,S} a_{L,S,J} a_{L,S,J}\} a_J(L,S) \quad .$$

The problem then is to calculate the coefficients $a_{L,S,J}$. In the following section this model is used to calculate the susceptibility of Pu(III) and Am(III).

Plutonium(III)

For small departures from LS coupling, the pure levels can be calculated and the mixing treated as a perturbation. For systems with more than two f electrons, the calculation of the energy of the different terms by the method of Condon and Shortly[51] is tedious. The tensor-operator and group-theoretical methods developed by Racah to simplify this problem have been treated in the Russell-Saunders approximation for $4f^n$ configurations with highest or next-highest multiplicities by Elliott et al.[52] In this notation each LS term is classified according to the quantum numbers (W, U, S, L, J). For Pu^{+3} the ground multiplet is $|{}^6H(110)(11)\rangle$, where (110)(11) are the W and U disignations. The nearest term that will interact with the ground multiplet by spin-orbit coupling is of the type ${}^4G$. Some of the electrostatic energy levels for the f^5 configuration have been calculated by Lammermann,[53] using F_k (Slater radial integrals) ratios obtained from 5f hydrogenic radial wave functions. She calculates that the separation of the lowest of the four ${}^4G$ terms and the ${}^6H$ term is 53.65 F_2, where F_2 is a Slater integral. Also, from her calculation the ${}^4G$ multiplet can be expanded, by using Racah notation, as

$$|^4G\rangle = 0.507\,|^4G(211)(20)\rangle + 0.115\,|^4G(211)(21)\rangle$$
$$- 0.723\,|^4G(211)(30)\rangle - 0.454\,|^4G(111)(20)\rangle .$$

The spin-orbit coupling in the LS limit is given by Elliott et al:[52]

$$\langle\psi\,|\,\zeta \sum_i s_i \ell_i\,|\,\psi'\rangle = \frac{\lambda\zeta}{2}\left\{J(J+1) - L(L+1) - S(S+1)\right\} .$$

They list spin-orbit splitting factors, λ, for 4f hydrogenic wave functions.

For the 5f functions:

$$\lambda = 0.336 \text{ for } |^4G\rangle ,$$
$$\lambda = 0.200 \text{ for } |^6H\rangle .$$

In the LS limit the energy levels will be as shown below.

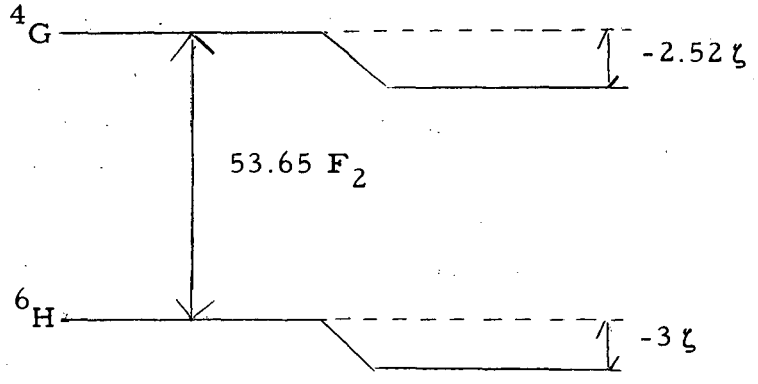

By comparison with the other actinide ions, a reasonable value for the parameter F_2 is 231 cm^{-1}, which is 2/3 of the F_2 for Sm^{+3}, the rare earth analogue; for ζ a reasonable value is 2400 cm^{-1}.[54] Therefore, in the LS limit the separation of the $|^4G\rangle$ and $|^6H\rangle$ is 1345 cm^{-1}. To calculate the mixing of the $|^4G\rangle$ and $|^6H\rangle$ terms the matrix element $\langle {}^6H_{5/2}\,|\,\zeta \Sigma \ell_i s_i\,|\,{}^4G_{5/2}\rangle$ is needed. Judd has calculated the spin orbit matrices,[54] $\langle {}^6H_{5/2}(110)(11)|\zeta \Sigma \ell_i s_i\,|\,{}^4G_{5/2}$ WU$\rangle$:

	$^4G_{5/2}$			
	(211)(20)	(211)(21)	(211)(30)	(111)(20)
$^6H_{5/2}(110)(11)$	0	0	$\sqrt{7}\,\zeta$	$\frac{2}{3}\sqrt{15}\,\zeta$

From these matrix elements and the expansion of the ^4G above one calculates

$$\left\langle {}^6H_{5/2} \left| \zeta \Sigma \vec{\ell}_i \cdot \vec{s}_i \right| {}^4G_{5/2} \right\rangle = 3.086\,\zeta = 7406\ \text{cm}^{-1}.$$

The mixing is given by the matrix:

	$\left\vert {}^6H_{5/2} \right\rangle$	$\left\vert {}^4G_{5/2} \right\rangle$
$\left\vert {}^6H_{5/2} \right\rangle$	$-\epsilon$	7406
$\left\vert {}^4G_{5/2} \right\rangle$	7406	$13545 - \epsilon$

The first-order calculation gives

$$0.915 \left\vert {}^6H_{5/2} \right\rangle + 0.403 \left\vert {}^4G_{5/2} \right\rangle .$$

The energy difference between the J = 7/2 and 5/2 levels is taken to be 3046 cm^{-1}, which is the separation of two groups of lines in the fluorescence spectrum of plutonium trichloride in lanthanum trichloride obtained by Cunningham et al.[55] Finally, if it is assumed that the eigenfunctions for the 5/2 and 7/2 levels are the same, then Eq. (9) for the susceptibility of Pu(III) becomes

$$\chi_{\text{mol.}} = \frac{0.1250}{XT} \; \frac{\{2.90x + 3.379 + [45.6x + 0.702]\, e^{-7x} + \ldots\}}{3 + 4\, e^{-7x}} ,$$

where

$$x = 626/T .$$

In Table XVII and Fig. 13 the susceptibility of Pu^{+3} obtained by Dawson from plutonium trichloride is compared with the susceptibility calculated with and without the correction for departures from Russell-Saunders coupling.[56] The results obtained by Dawson for plutonium trifluoride are also plotted in Fig. 13.

Table XVII. Comparison of experimental and calculated susceptibility of Pu(III).

	$Pu^{+3}(PuCl_3)$	$\|^6H\rangle$	$0.915\|^6H\rangle$ $0.403\|^4G\rangle$
T (°K)	$\chi_M \times 10^6$	$\chi_M 10^6$	$\chi_M 10^6$ (cgs units)
90	1607	1240	1567
200	887	694	829
300	658	544	628
334	606	512	587
373	571	485	549
397	548	471	529
428	525	454	507
457	515	441	490
491	484	428	472
520	464	417	458
548	462	409	447
583	472	400	434
300	659		

In the light of the many assumptions required to make the intermediate-field calculation, the agreement between theory and experiment is fairly good. If higher ^4G multiplets were included in the calculation, the resulting susceptibility would be raised slightly. However, because of the large possible errors in the assumed values of ζ and F_2, a more extensive calculation is not warranted. It is not surprising that

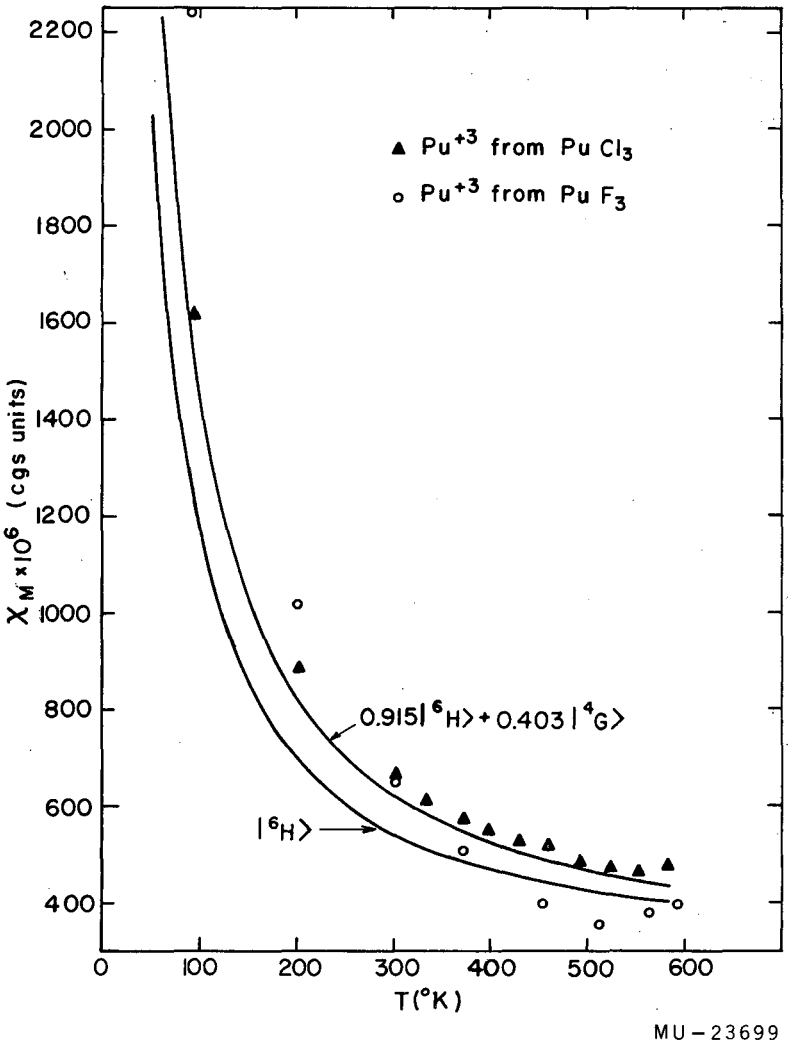

Fig. 13. Magnetic susceptibility of Pu(III).

this simple theory does not fit the experimental results for plutonium trifluoride. Because of the small size of the fluoride ion, there are undoubtedly plutonium-plutonium interactions that should be considered. It should be pointed out that the theory presented here will not produce a minimum in the susceptibility-versus-temperature curve until $T > 1000\ ^{o}K$. The evidence for a minimum in the chloride data is based on one point, but the trifluoride is more convincing. The present author cannot account theoretically for the apparent minimum between 500 and 550 ^{o}K in the experimental results.

Americium(III)

In americium the susceptibility clearly shows that the separation of the low-lying J levels is considerably larger than in europium, the rare earth analogue. The ground state is $^{7}F_{0}$, which is nonmagnetic. This gives rise to a unique condition in which the susceptibility results entirely from the second-order terms. The J = 1 level is not appreciably populated below 500 ^{o}K, and, therefore, the susceptibility calculated by using the above model is independent of temperature up to 500 ^{o}K.

$$\chi_{molar} = \frac{0.04345\ F_J}{h\nu(1;0)} \text{ cgs units.}$$

Gruber has measured the absorption spectrum of Am^{+3} in lanthanum trichloride and gives a separation of 2125 cm^{-1} between the J = 1 and 0 levles.[57] For his analysis of the ultraviolet absorption spectrum, he has calculated the following preliminary eigenvectors:

$$0.70\left|{}^{7}F_{1}\right\rangle + 0.65\left|{}^{5}D_{1}\right\rangle - 0.305\left|{}^{3}P_{1}\right\rangle ,$$

$$0.66\left|{}^{7}F_{0}\right\rangle + 0.73\left|{}^{5}D_{0}\right\rangle + 0.20\left|{}^{3}P_{0}\right\rangle .$$

In this calculation of the electrostatic energy levels 5f hydrogenic radial wave functions were assumed; also, ζ was assumed to be $2450 \pm 200\ cm^{-1}$ and $F_2(5f^6)$, 225 cm^{-1}.[58] Using these calculations,

one has

$$\chi_m = 682 \times 10^{-6} \text{ erg/gauss}^2, \text{ for } 5f^6 (Am^{+3}).$$

As the eigenvectors above were calculated by using perturbation theory, they probably are a lower limit, and the experimental results would be expected to lie above the calculated susceptibility. A comparison of the different results in Table XVIII shows agreement between experimental and calculated susceptibilities that is about as good as is to be expected, except for the measurements by Crane et al.[46] The experimental results show varying degrees of temperature dependence, depending on the matrix involved. There is no justification at this time for speculating as to the cause of this dependence, as it may result from any number of phenomena ranging from third-order terms neglected in the above treatment to free radicals or F centers produced by the decay of the americium. However, the discussion above shows that the magnetic susceptibility, calculated from a form of Van Vleck's equation which corrects for departures from Russell-Saunders coupling resulting from the spin-orbit interaction, is in agreement with the experimental results for Pu(III) and Am(III).

Table XVIII. Comparison of calculated and observed χ_m for Am^{+3}

Source	$\chi_m \times 10^{-6}$ (cgs units)
Calc.	682
AmF_3	566 ± 25^a
AmF_3 (Crane et al.)[46]	1040 ± 300^a
Am^{+3} on bead	716 ± 100^a
Am^{+3} in soln. (Howland and Calvin[45])	720

[a]Values include diamagnetic correction for Am^{+3}

VI. ELECTRICAL RESISTIVITY AS A FUNCTION OF TEMPERATURE AND PRESSURE

In collaboration with the high-pressure group under the direction of Professor Jura, a program to measure the electric resistance of several actinide metals from room temperature to 400° C and from 2 kilobars to 36 kilobars was started. The equipment has been described in detail elsewhere and will only be discussed briefly here.[59]

The apparatus is sketched in Fig. 14. The sample of metal (typically 0.2×0.2×0.7 mm) fills a hole in a silver chloride disk which is precoated with an acrylic plastic spray. The disk is surrounded by a pyrophylite ring which seals the sample cell when under high pressure. This assembly is then placed between platinum contacts in the cavity of a hardened steel anvil. A second anvil containing an insulated steel piston is put in place, and the apparatus is sealed with an insulated stainless steel cylinder. The loading of the apparatus is done in a nitrogen-filled dry box, and, if care is taken, the apparatus is not radioactively contaminated on the outside.

If extensive drying precautions were not taken, an actinide or rare earth metal pushed into the hole in the silver chloride disk would start to dissolve, with the evolution of bubbles. This reaction could be stopped by directing a stream of nitrogen on the disk. The cause of the reaction is not known, but it may be that enough water condenses by capillary action to hydrolyze the surface of the metal.

The anvil assembly is placed in a 100-ton hydraulic press, and the resistance across the faces is determined by using a four-lead measurement.

The apparatus has been used to determine the phase diagram of bismuth, lanthanum, neptunium, and plutonium.[59] Seven samples of americium have been run under varying conditions, but, in contrast to the elements above, the results were not reproducible. The initial isothermal compressions showed only a gradual decrease in the relative resistance up to 36 kilobars at 20°C. On decompression some samples showed a sharp rise in resistance around 20 kilobars,

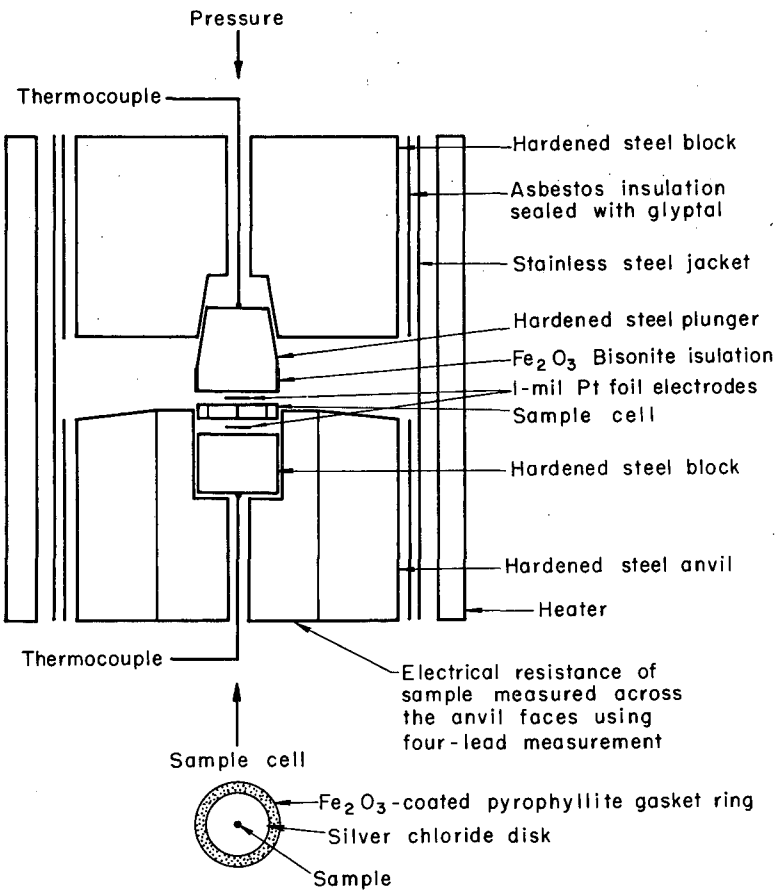

Fig. 14. High-pressure apparatus for resistivity measurements.

but others did not. Subsequent compressions were usually not reproducible. The measured resistance became less reproducible at higher temperatures. In attempts to do isobaric heatings, the resistance would rise irreversibly from a measured resistance of approximately 50 milliohms to several ohms (at which point the heat was removed) between 40°C and 80°C, depending on the pressure. After the runs the samples were still shiny in appearance, and x-ray diffraction patterns showed only lines corresponding to the dhcp phase. The diffraction lines generally were weaker after the run. By comparison with the resistance measured when samples of plutonium and bismuth of similar size were in the apparatus, the resistivity of americium metal is estimated to be 100 ± 50 micro-ohm centimeters. However, because of the lack of reproducibility in the measurements, no further conclusions can be drawn.

VII. DISCUSSION

The crystal structure and physical properties of americium metal presented above are markedly different from those of plutonium, the preceding element in the actinide series. For example, the melting point of americium is 355°C higher than that of plutonium. By far the most marked change is in the crystal structure. Plutonium has more allotropic forms than any other pure metal, and some of the phases have very complex structures, as do some phases of the two preceding elements, neptunium and uranium. Americium, on the other hand, has a close-packed structure similar to the early members of the rare earth series. The abrupt change in crystal structure of the actinides at americium is illustrated in Fig. 15.[60] The thermal expansion of these elements also changes at this point. Uranium, neptunium, and plutonium have large and very anisotropic coefficients of thermal expansion, whereas those of americium are very similar in sign and magnitude to the rare earths in general and to gadolinium in particular. Also, the only close-packed phase (δ) of plutonium has a negative coefficient of thermal expansion. In fact almost every physical property of plutonium is anomalous by comparison with other metals.

In Fig. 16 the heats of vaporization, atomic volumes, and melting points of the actinide metals are compared with those of the lanthanides and the second and third transition series elements.[39,60,61,62,63] A similar comparison of the magnetic propoerties of these metals is made in Fig. 17.[64,63,60] These graphs show that actinium and americium are very similar to the rare earth elements but that thorium, protactinium, uranium, neptunium, and plutonium have properties which are intermediate between those of the lanthanide and "d" transition series. The unusual crystal structures and magnetic, electrical, and dilatometric properties of these elements indicate that they are really unique in the periodic table, and there is little justification in classifying them simply as "f" or "d" transition elements.

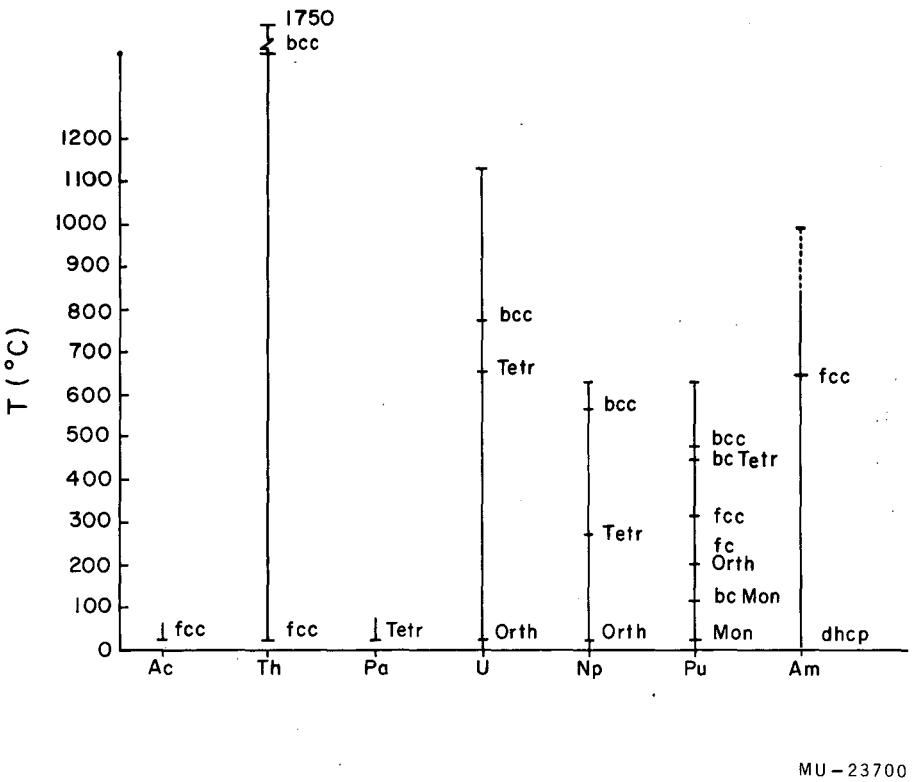

Fig. 15. Crystal structures of the actinide metals.

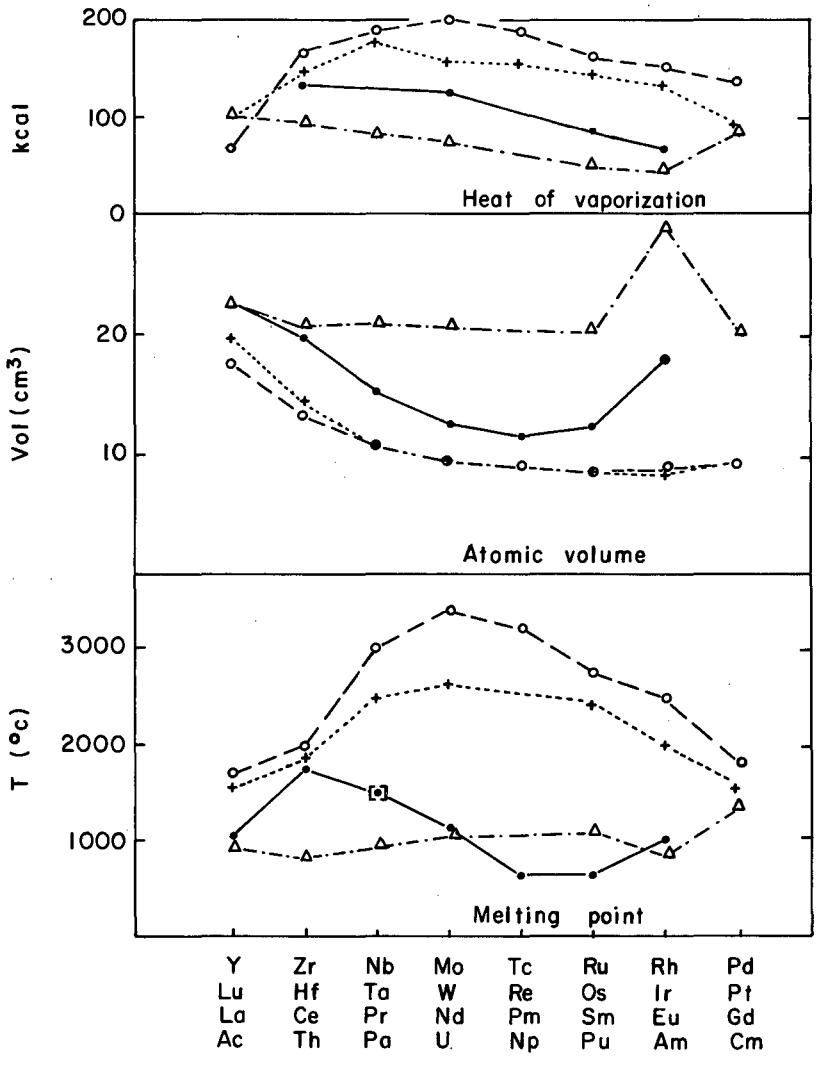

Fig. 16. Comparison of various properties of the transition elements, lanthanides, and actinides.

+ ····· + Y, Zr, Nb ···· 4d transition series
o — — — o Lu, Hf, Ta ···· 5d transition series
Δ — . — . Δ La, Ce, Pr ···· lanthanide series
● ——— ● Ac, Th, Pa ···· actinide series

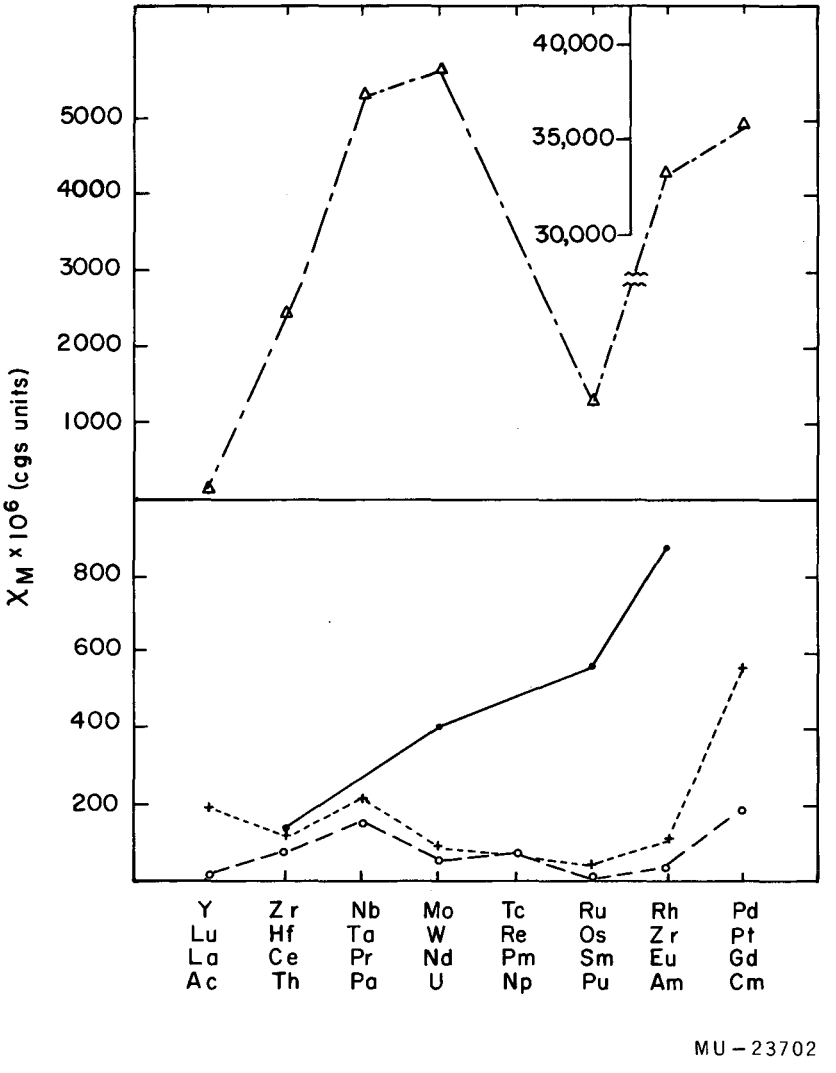

Fig. 17. Magnetic properties of "d" and "f" transition elements.

+ ····· + Y, Zr, Nb .... 4d transition series
o ___ o Lu, Hf, Ta .... 5d transition series
Δ – · – · Δ La, Ce, Pr.... 4f transition series
●———● Ac, Th, Pa.... 5f transition series

In other regions of the periodic table Pauling has shown that the trends in the metallic radii as a function of the atomic number can be used to infer the electronic configuration of metals.[65] Using these concepts, Zachariasen has predicted the metallic radii of the actinides for different configurations of d and f electrons.[65,67] His radii are based on two assumptions: (a) the change in the metallic radii on adding a d or an f electron is very different and can be predicted from the trends in the metallic radii observed in the d-transition and f-transition (lanthanide) series; (b) because thorium as a typically tetravalent element, it must be a d-transition element with no f electrons. Serious objections can be raised to both of these assumptions as applied to the early members of the actinide series.

First, the 5f electrons in the beginning of the actinide series are not as localized as the 4f electrons in the lanthanide series. A Hartree self-consistent field calculation for bcc uranium using a Wigner-Seitz approximation, shows that although the principal maximum for the 5f band is inside the (6s) (6p) shells, it is appreciable at the surface of the zone, and the 5f electrons must participate in bonding.[68] In the rare earths the 4f electrons do not take part in the bonding, as shown by the magnetic susceptibility of the metals which is similar to the susceptibility of the +3 ion. This fact indicates that the 4f electrons in the metal are like those in the free ion where their spin and orbital angular momentum couple to give a total angular momentum, J. This means that the effect on the metallic radii of adding 5f electrons to the early actinides cannot be obtained from similar additions of 4f electrons to the lanthanides. The situation is further complicated by the much larger interaction of the d and f bands. As a result of these complications, the effects of d and f electrons on the metallic radii in the early actinides is not as clearly separable as in the 5d and 4f transition series. A treatment such as that given by Zachariasen would predict the two possible limits of the metallic radii but would probably not give an accurate picture of the electronic configuration. As the middle of the actinide series is approached, the

5f electrons become more "internal" and participate less in bonding, and the change in the metallic radius resulting from the addition of a 5f electron would be expected to approach that observed in the lanthanide series.

Second, the assumption that thorium has to be a transition element is open to question. In Table XIX the heat of vaporization, atomic volume, melting point, and magnetic susceptibility of titantium, zirconium, hafnium, and thorium are listed. These properties show a definite trend on going from titanium to hafnium, but the value to thorium does not follow this trend. If thorium were clearly a d-transition element, one would expect these trends to continue from titanium to thorium. This does not imply that thorium contains a 5f electron, but in the light of the above discussion even smaller contributions from the 5f band might change the observed metallic radii.

Table XIX. Some properties of Ti, Zr, Hf, and Th

Element	$\Delta H_{v\,(298^{o}K)}$ (kcal)	at. vol (cm^3)	mp (^{o}C)	χ molar (10^{-6} cgs unit)
Ti	113	10.6	1800	153
Zr	146	14.3	1852	119
Hf	168	13.4	1977	75
Th	137	19.8	1750	130

However, existence of the "collapsed" cubic phase of cerium has been interpreted as resulting from promotion of a 4f electron to a 5d conduction band.[69] It would not be unreasonable to suppose that similar promotion would occur more readily in thorium, since the separation of the 5f → 6d level in Th(IV) is less than the 4f → 5d separation in Ce(IV). Metallic thorium may therefore be quite similar in the metallic state to the d-transition elements.

The separation of the 5f and 6d levels increases rapidly with increasing atomic number, however, and increasing departures from d-transition character must occur.

The work presented here indicates that americium is similar to the rare earths in its properties, and preliminary x-ray diffraction studies on curium also show the dhcp structure exhibited by La, Ce, Pr, Nd, and Am. (It should be pointed out that the magnetic susceptibility of americium metal, although it follows the trend in the susceptibility observed in the beginning of the actinide series, is also compatible with the calculated susceptibility of a $5f^6$ configuration. Therefore, without further evidence in the form of susceptibility data for curium metal, the observed susceptibility of americium metal cannot be used as evidence for the rare-earth-like character of americium metal.) The experimental results available at this time indicate that actinium, americium, and curium metals have properties similar to those of the rare earth metals, and their metallic radii can be used to construct a curve of metallic radii versus atomic number for a 5f transition series.

The value for americium, derived from this work, presumably is quite accurate. The value for actinium has been questioned (Zachariasen[66]), although Farr et al. prepared lanthanum by the same technique and obtained the accepted metallic radius for this metal (fcc phase).[70] Their value for actinium is very close to that of lanthanum.

The curium radius is highly questionable, since it was obtained from diffraction data on two samples containing only 80 and 90 mol% curium with the following impurities: (a) 7 mol% aluminum, 2 mol% calcium, 8 mol% sodium, 2 mol% magnesium, and 4 mol% lithium, (b) 4 mol% aluminum, 1 mol% sodium.

With these reservations in mind, however, a curve of metallic radii versus atomic number for a 5f transition series can be constructed. By using the method of Zachariasen a 6d transition series curve can be

calculated. To do this the radius of actinium is compared with that of yttrium to obtain a scale factor of 1.04. On the assumption that the percent change in the radii across the rubidium series is similar to that of a 6d transition series, the metallic radii for the 6d transition series can be calculated by multiplying the observed radii in the rubidium series by the scale factor of 1.04. The results are shown in Fig. 18. The curves are highly tentative, but are compatible with the elements thorium, protactinium, uranium, neptunium, and plutonium being intermediate between d and f -transition elements as discussed above. The curves given by Zachariasen have exactly the same shape but are shifted upwards by 0.13Å. His curves imply that thorium, protactinium, and uranium may be classified as 6d transition elements, which is not compatible with the properties shown in Figs. 16 and 17.

Qualitatively the complex nature of the early actinide metals can be understood by considering the electronic configuration of the gaseous atoms of the actinides and lanthanides as determined by atomic beam resonance studies. These are presented in Table XX. (The configurations show the electrons above the radon and xenon cores respectively.) The 6d electrons are bound more tightly than the 5f electrons, and, as a result of this, there is a d electron in the gaseous atoms up to plutonium. The relative binding energies of the last competing electron in the lanthanides and the actinides are presented in Fig. 19 (taken from Cabezas[71]). In the lanthanide elements the f band is lower in energy and more "internal," thus leading to relatively simple close-packed crystal structures and normal physical properties. In the actinides the d and f bands are very close in energy and probably overlap, giving rise to a much more complicated electronic structure which is the cause of the complex crystal structures and atypical physical properties observed between protactinium and plutonium. This also leads to more than the normal three bonding electrons which probably accounts for the smaller atomic volumes and high heats of vaporization in this region of the periodic table.[72] At americium the f band is lowest and properties similar to those of the lanthanides are observed.

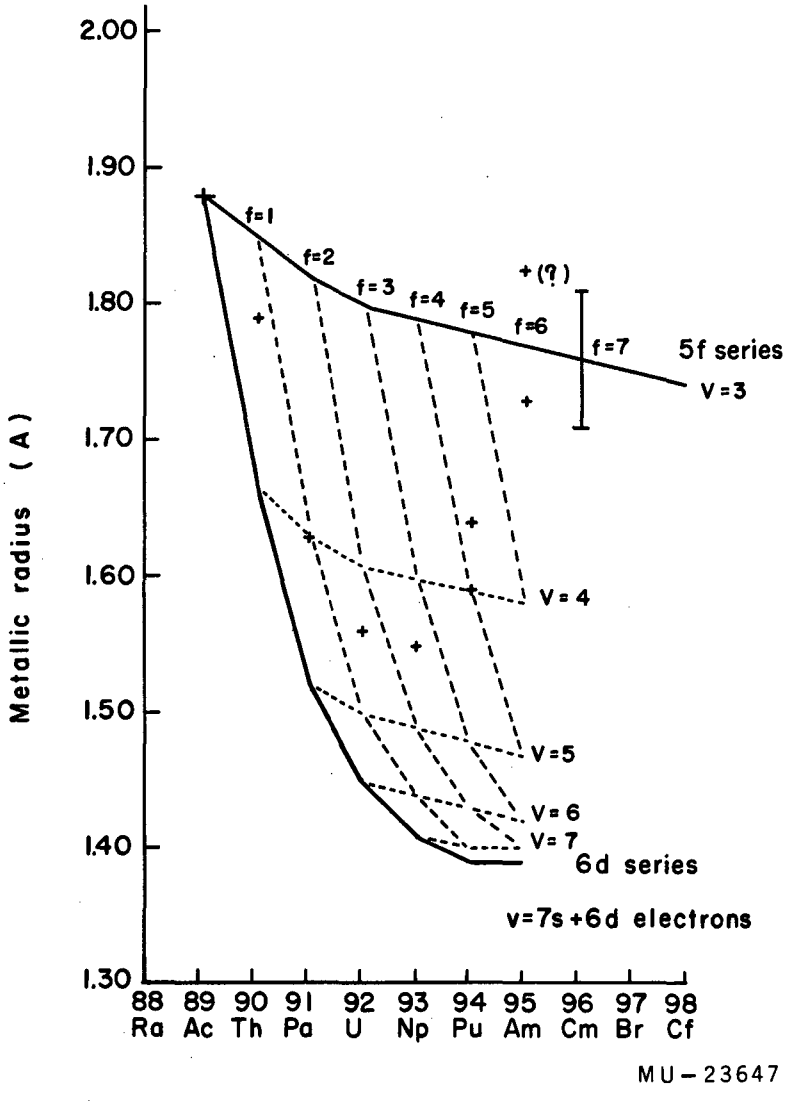

Fig. 18. Predicted radii for the actinide metals.

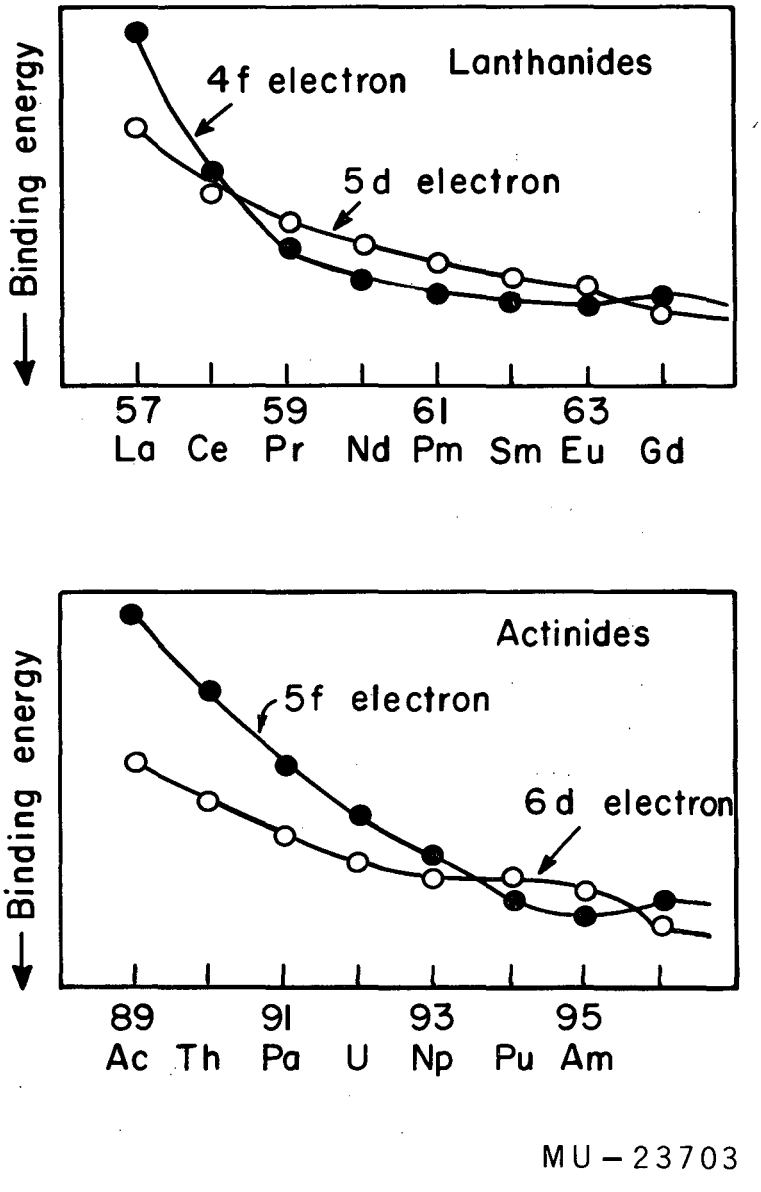

Fig. 19. Qualitative comparisons of the binding energies of the last competing electron in the lanthanides and actinides.

Table XX. Electronic configuration of the gaseous atoms of the actinide and lanthanide elements (Ref. 70).

Ac	$6d7s^2$	La	$5d6s^2$
Th	$6d^2 7s^2$	Ce	$(4f5d6s^2)$
Pa	$5f^2 6d7s^2$	Pr	$4f^3 6s^2$
U	$5f^3 6d7s^2$	Nd	$4f^4 6s^2$
Np	$5f^4 6d7s^2$	Pm	$4f^5 6s^2$
Pu	$5f^6 7s^2$	Sm	$4f^6 6s^2$
Am	$5f^7 7s^2$	Eu	$4f^7 6s^2$
Cm	$5f^7 6d7s^2$	Gd	$4f^7 5d6s^2$

The theoretical calculation of the physical properties of the actinides presents an awesome task although several notable attempts have been made.[68, 73, 74] It is probable, however, that a real understanding of these elements will come from careful studies of the physical properties of different systems of alloys. Of more immediate concern is the changes in the physical properties produced by small amounts of anionic impurities, and a study of these effects is one of the most important lines of research that can be undertaken in this field in the near future.

ACKNOWLEDGMENTS

It is a pleasure for me to express my thanks to Professor Burris B. Cunningham. His constant presence and willingness to help have provided encouragement, and his suggestions invariably have pointed to the core of the problem.

I wish to thank Dr. James C. Wallmann, whose help with experimental problems and whose moral support have greatly aided my work.

My thanks to Dr. Sherman Fried, whose broad interests have been both an inspiration and aid on the road to a Ph.D. degree.

I would like to thank Dr. John D. Axe, Dr. Brian R. Judd, and Mr. Tom Parsons for many helpful suggestions. Also, I wish to thank Dr. Hugo Schumacher and John Burnett for helping with some of the preliminary magnetic susceptibility measurements. A special vote of thanks is to be given to Mr. George Shalimoff for making the countless spectrographic analyses. Also, I wish to thank Dr. P.W. Montgomery for making the high-pressure measurements and Dr. Melvin H. Mueller for providing the lattice parameter program.

The help in the laboratory of Miss Lilly Goda, our technician, and Mrs. Gertrude Bolz, the health chemistry monitor, has been invaluable.

My thanks to Mr. Bert Watkins and Mr. Hap Hagopian for their expert engineering advice and to Mr. Harry Powell for making the glass apparatus used in this work. The help of the Health Chemistry group was greatly appreciated.

The greatest gratitude is due my wife, who not only kept up my spirits but also helped materially in many of the measurements and calculations.

I would like to express my appreciation to the University of California for the award of a U.S. Rubber Company fellowship and a Dow Chemical Company fellowship.

This work was done under the auspices of the United States Atomic Energy Commission.

REFERENCES

1. E. F. Westrum, Jr., and L. Eyring, J. Am. Chem. Soc. 73, 3396 (1951).
2. S. C. Carniglia and B. B. Cunningham, J. Am. Chem. Soc. 77, 1502 (1955).
3. H. R. Lohr and B. B. Cunningham, J. Am. Chem. Soc. 73, 2025 (1951).
4. P. Graf, B. B. Cunningham, C. H. Dauben, J. C. Wallmann, D. H. Templeton, and H. Ruben, J. Am. Chem. Soc. 78, 2340 (1956).
5. L. B. Asprey (Los Alamos Scientific Laboratory), Los Alamos, New Mexico, private communication, 1958.
6. F. Trombe, Rev. mét. 52, 2 (1956).
7. S. Fried, E. F. Westrum, Jr., H. L. Baumback, and P. L. Kirk, J. Inorg. and Nuclear Chem. 5, 182 (1958).
8. J. C. Wallmann and B. B. Cunningham, UCRL-8369, July 1958, in Chemistry Division Semiannual Report.
9. A. H. Daane, O. H. Dennison, and F. H. Spedding, J. Am. Chem. Soc. 75, 2272 (1953).
10. J. J. Hanak, High Temperature Crystal Crystal Structures of the Rare Earth Metals (Thesis), Iowa State College, Ames, Iowa, 1959.
11. A. F. Wells, Structural Inorganic Chemistry, 2nd Ed. (Oxford University, Clarendon Press, London (1950).
12. Estimated from: A. Glassner, The Thermochemical properties of the Oxides, Fluorides, and Chlorides to 2500°K, ANL-5750, 1957.
13. R. E. Honig, RCA Review, 195, June 1957.
14. L. Brewer, The Fusion and Vaporization Data of the Halides, in The Chemistry and Metallurgy of Miscellaneous Materials (McGraw-Hill, New York, 1950), paper 7.
15. K. Naito, A Method of Purification of Americium, UCRL-8748, Dec. 1959.
16. B. B. Cunningham, Submicrogram Methods in Studies of the Synthetic Elements, to be published in the Microchemical Journal.

17. R. H. Perkins, Tantalum Annealing and Degassing and Hardness Effects of Dissolved Gases, LA-2136, May 1957.
18. O. S. Edwards and H. Lipson, Proc. Roy. Soc. (London) A180, 268 (1942).
19. A. J. C. Wilson X-ray Optics (Methuen and Company, London, 1949).
20. A. H. Daane and F. H. Spedding, Abstract of paper given at the fall meeting of the American Chemical Society, Chicago, Illinois, September 1958, paper No. 58, Division of Physical Chemistry.
21. F. H. Ellinger and W. H. Zachariasen, J. Am. Chem. Soc. 75, 5650 (1953).
22. W. H. Zachariasen, Acta Cryst. 2, 388 (1949).
23. Yumi Akimoto, in Chemistry Division Semiannual Report UCRL-9093, 1959.
24. P. Graf, in Chemistry Division Quarterly Report, UCRL-3415.
25. J. C. Wallmann (Lawrence Radiation Laboratory), private communication, 1958.
26. W. H. Zachariasen, in 14a National Nuclear Energy Series (McGraw-Hill Book Co., Inc., New York) Ch. 18 IV.
27. H. S. Peiser, H. P. Rooksby, and A. J. C. Wilson ed., X-ray Diffraction by Polycrystalline Materials (Chapman and Hall, London, 1960 Ch. 9 and 10.
28. M. J. Buerger, N. W. Buerger, and F. G. Chesley, Am. Mineral. 28, 285 (1943).
29. W. Parrish and E. Cisney, Philips Tech. Rev. 10, 157 (1948).
30. Ref. 27, Ch. 15.
31. M. J. Buerger, X-ray Crystallography (Chapman and Hall, London, 1942).
32. A. Taylor and H. Sinclair, Proc. Phys. Soc. (London) 57, 126 (1945).
33. J. B. Nelson and D. P. Riley, Proc. Phys. Soc. (London) 57, 160 (1945).
34. M. U. Cohen, Rev. Sci. Instr. 6, 68 (1935).
35. J. B. Hess, Acta Cryst. 4, 109 (1951).

36. M. H. Mueller and LeRoy Heaton, Determination of Lattice Parameters with the Aid of a Computor, ANL-6176, March 1961.
37. M. H. Mueller, LeRoy Heaton, and K. T. Miller, Acta Cryst. 13, 828 (1960).
38. R. W. G. Wyckoff, Crystal Structures (Interscience Publishers, New York 1948).
39. Handbook of Chemistry and Physics 42nd ed. (Chemical Rubber Publ. Co., Cleveland, 1960).
40. C. R. Houska, B. L. Averback, and M. Cohen, Acta Met. 8, 81 (1960).
41. B. B. Cunningham, J. Chem. Educ. 36, 31 (1959).
42. P. Cosse, J. Inorg. & Nuclear Chem. 14, 127 (1960).
43. L. C. Jackson, Phil. Trans. Roy. Soc. London A224, 1 (1924).
44. G. Foex, Tables de constantes et données numériques-7: Constantes sélectionnées, diamagnétisme et Paramagnétisme (Masson et Cie., Paris, 1957).
45. J. J. Howland, Jr., and M. Calvin, J. Chem. Phys. 18, 239 (1950).
46. W. W. T. Crane, J. C. Wallmann, and B. B. Cunningham, The Magnetic Susceptibilities of some Compounds of Americium and Curium, UCRL-846, Aug. 1950.
47. F. H. Spedding J. Am. Chem. Soc. 54, 2596 (1932).
48. Estimated from P. W. Selwood, Magnetochemistry, 2nd Ed. (Interscience Publishers, Inc. New York, 1956).
49. J. H. Van Vleck. The Theory of Electric and Magnetic Susceptibilities (Oxford, 1932).
50. B. R. Judd and I. P. K. Lindgren, Theory of Zeeman Effects in the Ground Multiplets of Rare Earth Atoms, UCRL-9188 May 1960.
51. E. W. Condon and G. H. Shortley, The Theory of Atomic Spectra (Cambridge University Press, London, 1935).
52. J. P. Elliott, B. R. Judd, and W. A. Runciman, Proc. Roy Soc. (London) A240, 509 (1957).
53. H. Lammermann, (Lawrence Radiation Laboratory), Private communication 1961.

54. The Author is indebted to Dr. Brian R. Judd for these values and for aid in the calculation.

55. B. B. Cunningham, D. M. Gruen, J. G. Conway, and R. D. McLaughlin, J. Chem. Phys. 24, 1275 (1956).

56. J. R. Dawson, C. J. Mandleberg, and D. Davies, J. Chem. Soc. (London) 2047 (1951).

57. J. B. Gruber, An Analysis of the Infrared Absorption Spectrum of $Am^{+3}(5f^6)$ in $LaCl_3$ UCRL-9584), J. Chem. Phys. (in press, 1961).

58. J. B. Gruber (Lawrence Radiation Laboratory), private communication, 1961.

59. P. W. Montgomery, Phase Relationships and Sintering Properties of Materials at High Pressures, (Thesis), University of California, Berkeley, 1960.

60. J. J. Katz and G. T. Seaborg, The Chemistry of the Actinide Elements (Methuen and Co., London, 1957).

61. D. R. Stull and G. C. Sinke, Thermodynamic Properties of the Elements, (American Chemical Society, Washington, D. C., 1956).

62. G. N. Lewis & M. Randall, Thermodynamics (McGraw-Hill Book Co. New York, 1961.

63. K. A. G. Schneidner, Critical Review of the Alloy Systems of the Rare Earth, Scandium, and Yttrium Metals, Preprint of AEC-LA Report).

64. C. J. Kriessman and H. B. Callen, Phys. Rev. 94, 837 (1954).

65. L. Pauling, The Nature of the Chemical Bond (Cornell University Press, Ithaca, N. Y. 1960).

66. W. H. Zachariasen, The Crystal Structure of Plutonium Metal, Paper presented at the Plutonium Conference, Chicago, 1957.

67. W. H. Zachariasen, Acta Cryst. 5, 660 (1952).

68. E. Cicely Ridley, Proc. Roy. Soc. (London) 247A, 199 (1958).

69. A. F. Schuch and J. H. Sturdivant, J. Chem. Phys. 18, 145 (1950).

70. J.D. Farr, A.L. Giorgi, R.K. Money, and M.G. Bowman, The Crystal Structure of Actinium Metal and Actinium Hydride LA-1545 (AEC report) April, 1953.

71. A.Y. Cabezas, Electronic and Nuclear Properties of Some Radioactive Rare-Earth Elements, (Thesis), UCRL-9346, Aug. 1960.

72. B.B. Cunningham, Comparative Chemistry of the Lanthanide and Actinide Elements, Paper presented at the XVII International Congress of Pure and Applied Chemistry, Munich, 1959.

73. G.W. Lehman, Electronic Structures of the Heavy Metals, in Progress in Nuclear Energy, Series V: Metallurgy and Fuels (Pergamon Press, London, 1959), Ch. 10.

74. J. Friedel, J. Phys. Chem., Solids 1, 175 (1957).

75. W.A. Chupka, M.G. Ingram, and R.F. Porter J. Chem. Phys. 24, 792 (1956).

This report was prepared as an account of Government sponsored work. Neither the United States, nor the Commission, nor any person acting on behalf of the Commission:

A. Makes any warranty or representation, expressed or implied, with respect to the accuracy, completeness, or usefulness of the information contained in this report, or that the use of any information, apparatus, method, or process disclosed in this report may not infringe privately owned rights; or

B. Assumes any liabilities with respect to the use of, or for damages resulting from the use of any information, apparatus, method, or process disclosed in this report.

As used in the above, "person acting on behalf of the Commission" includes any employee or contractor of the Commission, or employee of such contractor, to the extent that such employee or contractor of the Commission, or employee of such contractor prepares, disseminates, or provides access to, any information pursuant to his employment or contract with the Commission, or his employment with such contractor.